Int J Earth Sci (Geol Rundsch) (2009) 98:627–650
DOI 10.1007/s00531-007-0269-9

ORIGINAL PAPER

The Oligo-/Miocene Qom Formation (Iran): evidence for an early Burdigalian restriction of the Tethyan Seaway and closure of its Iranian gateways

M. Reuter · W. E. Piller · M. Harzhauser · O. Mandic · B. Berning · F. Rögl · A. Kroh · M.-P. Aubry · U. Wielandt-Schuster · A. Hamedani

Received: 14 March 2007 / Accepted: 11 October 2007 / Published online: 28 November 2007

Abstract In the central Iranian Esfahan-Sirjan and Qom basins sedimentation of the Oligo-/Miocene Qom Formation took place on extensive mixed carbonate–siliciclastic ramps. During this time, both basins were positioned at the Eurasian margin of the Tethyan Seaway, which connected the western and eastern regions of the Tethys Ocean at least until the late Burdigalian. During the so-called Terminal Tethyan Event the Tethyan Seaway was then closed due to the collision of the African/Arabian and Iranian/Eurasian plates. Facies analysis of the sedimentary record of both basins indicates paleoenvironments ranging from terrestrial to open marine settings, including mangrove, restricted inner shelf lagoon, seagrass meadow, reefal, and deeper offshore environments. Recognition of eight depositional sequences and elaboration of an integrated biostratigraphic framework (calcareous nannoplankton, planktic and larger benthic foraminifers, gastropods, and pectinids) allow us to construct a basin-spanning stratigraphy. The assignment of the recognized sea-level lowstands to the Ru 3 to Bur 3 lowstands of the global sea-level curve enables a comparison with time-equivalent sections from the Zagros Basin, which was part of the African/Arabian Plate on the opposing southern margin of the Tethyan Seaway. The so calibrated sections display restrictions of the Tethyan Seaway and interruption of the south Iranian gateways between the Qom Basin and the Proto-Indopacific in relation to ongoing plate collision during the early Burdigalian.

Keywords Qom Formation · Stratigraphy · Terminal Tethyan Event · Tethyan Seaway · Iran

M. Reuter (✉) · W. E. Piller · B. Berning
Institute of Earth Sciences, Graz University,
Heinrichstrasse 26, 8010 Graz, Austria
e-mail: markus.reuter@uni-graz.at

M. Harzhauser · O. Mandic · F. Rögl · A. Kroh
Natural History Museum Vienna,
Burgring 7, 1010 Vienna, Austria

M.-P. Aubry
Department of Geological Sciences, Rutgers University,
610 Taylor Road, Piscataway, NJ 08854-8066, USA

U. Wielandt-Schuster
Landesamt für Geologie, Rohstoffe und Bergbau
Baden-Württemberg, Albertstrasse 5,
79104 Freiburg, Germany

A. Hamedani
Geology Department, Esfahan University,
81744 Esfahan, Iran

Introduction

Sediments of the Qom Formation have an extensive distribution in northern and central Iranian Qom and Esfahan-Sirjan basins (Stöcklin and Setudehina 1991) (Fig. 1) and comprise thick successions of marine marls, limestones, gypsum and siliciclastics. After oil was discovered in porous bioclastic limestones in 1934 (Mostofi and Gansser 1957; Abaie et al. 1963; Rosenberg 1975) the Qom Fm. moved into the focus of scientific research. Historical investigations of the Qom Fm. reach back to Furrer and Soder (1955), who established the type locality near the town of Qom and defined six lithostratigraphic units (a- to f-Members: a-Member = basal limestone, b-Member = sandy marls, c-Member = alternating marls and limestones, d-Member = evaporites, e-Member = green marls, f-Member = top limestone). Whereas Bozorgnia (1966) recognized two sedimentary cycles in the Qom Fm. at its type area, Nogole-Sadat (1985) identified a third

sedimentary cycle. Biostratigraphic studies on larger foraminifers were carried out by Rahaghi (1973, 1976, 1980), who assigned an Oligo-/Miocene age to the Qom Fm. More recently, a paleoenvironmental reconstruction based on microfacies analysis was attempted for the f-Member (Okhravi and Amini 1998). However, geological research of the Qom Fm. mostly remained limited to the Qom Basin and the f-Member because of economic interests.

An Austrian/German cooperation-project, which aimed at a paleobiogeographic reconstruction of the eastern Mediterranean to western Indo-Pacific regions from the Late Oligocene to Early Miocene, integrated data from faunal analyses of the Qom Fm. from the Qom and Esfahan-Sirjan basins (Harzhauser et al. 2002; Harzhauser 2004; Schuster and Wielandt 1999; Mandic 2000). Within this project, basic biostratigraphic data from the Qom Fm. outside the Qom Basin were already published by Schuster and Wielandt (1999). However, up to now no satisfactory stratigraphic framework exists that allows a correlation of the Qom Fm. between both basins, which is crucial for paleobiogeographic as well as for oil exploration aspects. The aim of this study is therefore to bridge this gap by the development of a high-resolution stratigraphy using integrated biostratigraphic and sequence stratigraphic approaches.

Geological setting and location of studied sections

The tectonic units of central Iran originated during subduction and final collision of the African/Arabian Plate with the Iranian Plate, the process of which already started during the Mesozoic (Coleman-Sadd 1982). An important effect of the collision of these plates with far-reaching paleobiogeographic and -oceanographic consequences was the closure of the Tethyan Seaway (Fig. 2) during the Miocene. The so-called Terminal Tethyan Event (TTE) marks the termination of migration of marine biota and exchange of tropical waters between the eastern Mediterranean and the western Indo-Pacific Tethys (Harzhauser et al. 2007). However, the exact timing of the TTE is still debated. Adams et al. (1983) infer an Aquitanian age, while several other authors proposed a Burdigalian age (Rögl and Steininger 1983, 1984; Rögl 1997, 1999; Whybrow 1984; Robba 1986; Harzhauser et al. 2002). Jones (1999) discussed intermittent episodes of separation of the Eastern from the Western Tethys during Early and Middle Miocene sea-level lowstands and a final closure not until the end of the Middle Miocene. Another effect of the plate collision was the formation of a fore-arc (Esfahan-Sirjan Basin) and a back-arc basin (Qom Basin) on the Iranian Plate at the north-eastern margin of the Tethyan Seaway (Figs. 1, 2). These basins are separated by a volcanic arc system (Fig. 1), which developed during Eocene times (Stöcklin and Setudehina 1991). In both foreland basins the marine sedimentation of the Qom Fm. began during the Oligocene and continued until the Early Miocene (Rahaghi 1973, 1976, 1980). All sections presented in this paper comprise deposits of the Qom Fm., which is lithostratigraphically defined as a marine succession bounded by the underlying Lower Red Formation and the overlying Upper Red Formation, both consisting of continental redbeds (Stöcklin and Setudehina 1991).

Within this study, two sections were investigated in the Esfahan-Sirjan fore-arc basin (sections of Abadeh and Zefreh) and two in the Qom back-arc basin (sections of Qom and Chalheghareh) (Fig. 1). The Esfahan-Sirjan fore-arc basin strikes in a SE-NW direction about 550 km parallel to the south-western margin of the Iranian Plate. To the NE it is bounded by the Kuhrud Mountains, whereas its south-western margin is formed by the Zagros Mountains which are part of the Arabian Plate. Both investigated sections are incomplete. Section Abadeh represents the lower part of the Qom Fm. and has a thickness of 164 m, while the totally 260 m thick Zefreh section is a representative for its upper part and is situated in a more marginal position of the basin than Abadeh. The section of Abadeh is located 40 km NNE of the town Abadeh and can be reached by a track which turns off from the main road to Esfahan approximately 6 km NNW of Abadeh. This track runs for about 40 km in N to NE direction until it reaches some conspicuous E–W running hills. The section was measured at the flank of the first hill NE of the track (Fig. 1d). The position of the base of the section is 31°30.61′N, 52°43.99′E. Section Zefreh is located 50 km ENE of Esfahan, about 20 km north of the road from Esfahan to Nain, and west of the railroad track from Esfahan to Kashan. The section is situated at the NE wing of an anticline (Fig. 1c) and is composed of two partial sections (Zefreh A, Zefreh B). Zefreh A covers the stratigraphically older part of the section. Its base is located at 32°56.59′N, 52°08.39′E. Zefreh B is located 500 m further east.

The Qom back-arc basin extends along the Elburz Mountains from Semnan in the east to the Kuhrud Mountains NW of Tehran, and from there about 650 km to the south. The here measured section of Qom is located in the type area of the Qom Fm. (Furrer and Soder 1955) and near the depocenter of the Qom Basin, where the formation reaches a maximum thickness of about 1,000 m. The outcrop is situated 100 km south of Tehran and c. 10 km SW of the city of Qom at the southern flank of a large, E–W oriented anticline with steeply inclined and overturned beds (Figs. 1a, 3a). Its position (top of the section) is 34°38.41′N, 50°42.76′E. The Chalheghareh section has a more nearshore position within the Qom Basin, which is reflected in the lower thickness of the Qom Formation

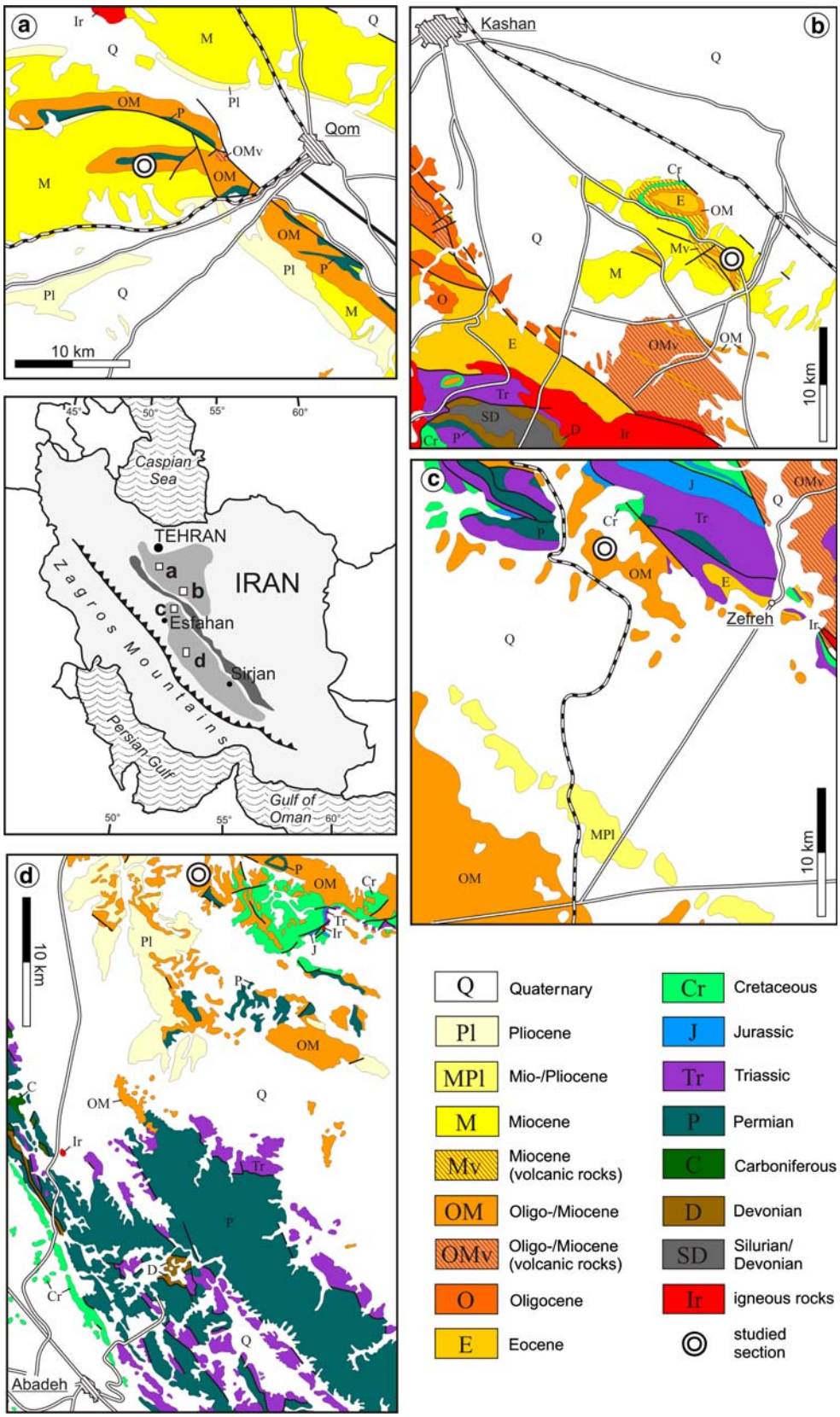

Fig. 1 Localities and geological maps (modified from Zahedi 1978; Amidi 1983; Amidi and Zahedi 1991; Emami 1991) of the studied locations in central Iran. The Esfahan-Sirjan Basin and the Qom Basin are highlighted in *light gray* and the volcanic arc as a *dark gray* field in the overview map. The *serrated line* indicates the Zagros thrust fault. Qom Basin: **a** Qom locality, **b** Chalheghareh locality. Esfahan-Sirjan Basin: **c** Zefreh locality, **d** Abadeh locality

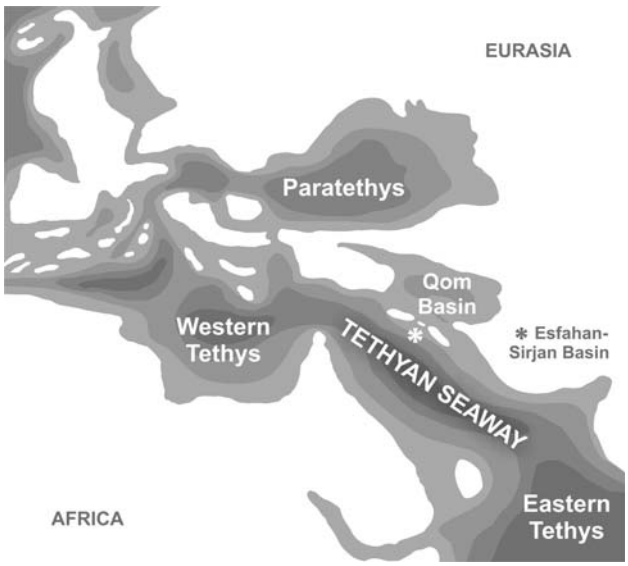

Fig. 2 Late Oligocene paleogeography of the Tetyan Seaway and adjacent regions (modified from Harzhauser and Piller 2007)

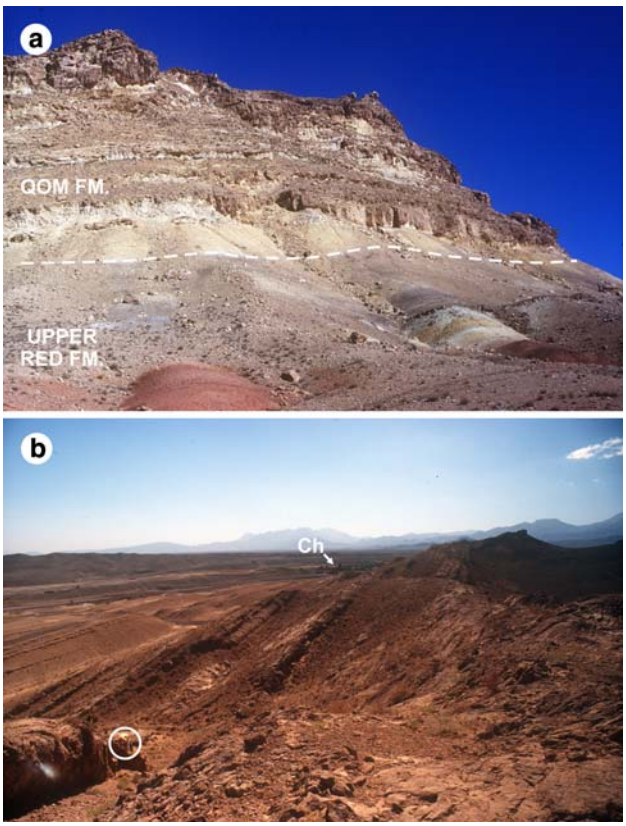

Fig. 3 View of sections Qom and Chalheghareh in the Qom Basin. **a** Overturned beds in the upper segment of the Qom section. The continental redbeds of the Upper Red Formation are topped by bioclastic limestones of the f-Member forming a steep cliff. **b** Section Chalheghareh at the NE wing of an anticline NW of the village Chalheghareh (*Ch*). Person for scale (*white circle*)

(340 m). It is located directly west of the road from Esfahan to Kashan, 45 km north of Natanz, and NW of the small village Chalheghareh, where the Qom Fm. is exposed in an anticline. The section was measured at the NE wing (Figs. 1b, 3b) and the position of the base of the section is 33°46.99′N, 51°43.76′E.

Sedimentary facies

The numbers provided in the following descriptions and interpretations of the studied sections refer to consecutively numbered beds in Figs. 4, 6, 7, 8 and 9.

Abadeh section

The Abadeh section (Fig. 4) starts with the contact between reddish, continental conglomerates of the underlying Lower Red Fm. and the overlying Qom Fm. Although the contact is usually not exposed due to a cover of alluvial scree, nummulitic limestones were found in small isolated outcrops that are located slightly above the contact between the Lower Red and Qom formations.

The base of the Qom Fm. (1–13) is dominated by brown, gray and red marls, and by argillaceous limestones. Characteristic for this part of the section are *Nummulites* mass occurrences (*Nummulites sublaevigatus*) with abundant *Ophiomorpha* burrows (e.g., 1, 13). In the upper part of this unit, thin (0.1–0.3 m) beds of fine-grained, partly laminated calcareous sandstones and grainstones occur that alternate with thicker (0.25–3.1 m) beds of argillaceous limestones and marls. Tests of larger foraminifers (*Nummulites*, *Operculina*, heterosteginids, *Amphistegina*) are distributed in the marly package. Associated rich assemblages of smaller benthic foraminifers are dominated by *Almaena*, *Neoeponides*, *Rosalina*, *Nonion*, *Cibicidoides*, and *Lobatula*. Plankton is scarce. Solitary corals, bivalves and gastropods (*Turritella* and cerithiopsids, see Harzhauser 2004) are co-occurring (solitary coral assemblage *sensu* Schuster and Wielandt 1999).

Upsection (14–19) a distinct shift in rock color from red/brown to gray/green occurs, yet without significant changes in lithology. Marly sediments continue to be present, containing now lepidocyclinids for the first time [*Lepidocyclina* (*Eulepidina*) *formosoides*, *L.* (*E.*) *favosa*, *L.* (*Nephrolepidina*) *morgani*-type] and small turritellids. Planktic foraminifers are common and represented by *Globigerina praebulloides*, *Gg. ciperoensis*, *Gg. angulioficinalis*, *Gg. ouachitaensis*, *Globigerinella obesa*, *Paragloborotalia pseudocontinuosa*, *Pgr. opima opima*, *Pgr. opima nana*, *Globorotaloides testarugosus*, *Tenuitellinata angustiumbilicata*, *Tenuitella insolita*, *T. gemma*, and *Cassigerinella chipolensis*.

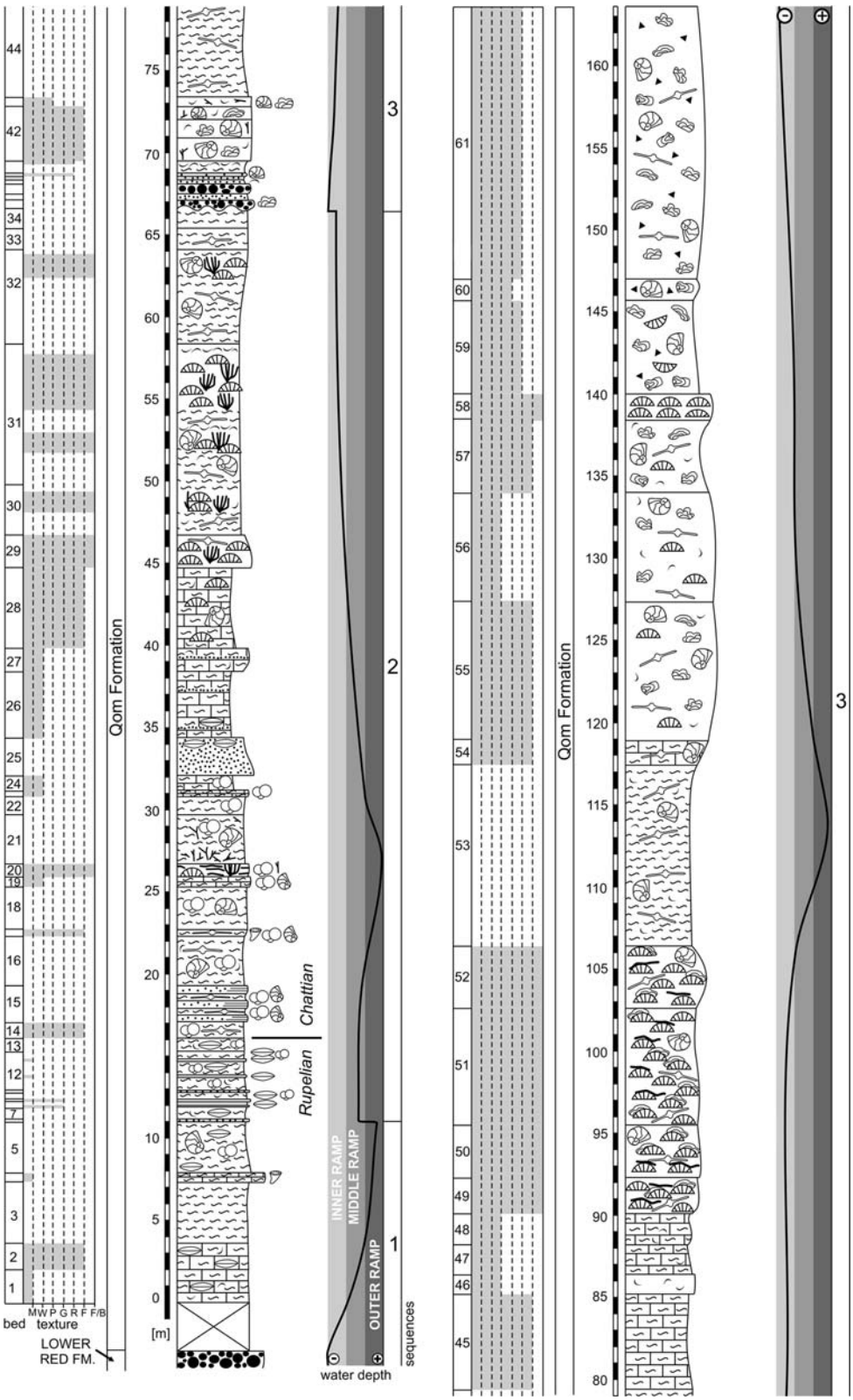

Fig. 4 Abadeh section. From *left* to *right* consecutive numbers of sampled beds, texture, formation names, scale in meters, lithological succession, chronostratigraphy, water depth trend, and number of identified depositional sequences. The legend applies also for the measured sections Zefreh, Qom and Chalheghareh (Figs. 6, 7, 8, 9)

A distinct coral framestone horizon follows (20), which thins out laterally but is traceable for several hundreds of meters. It is dominated by foliaceous (*Leptoseris*) and thin branching forms (*Stylophora*) with minor numbers of massive dome-shaped colonies (mostly meandroid faviids; *Leptoseris-Stylophora* assemblage sensu Schuster and Wielandt 1999). Associated planktic foraminifers belong to *Pgr. opima opima*, *Gg. angulioficinalis*, *Gg.*

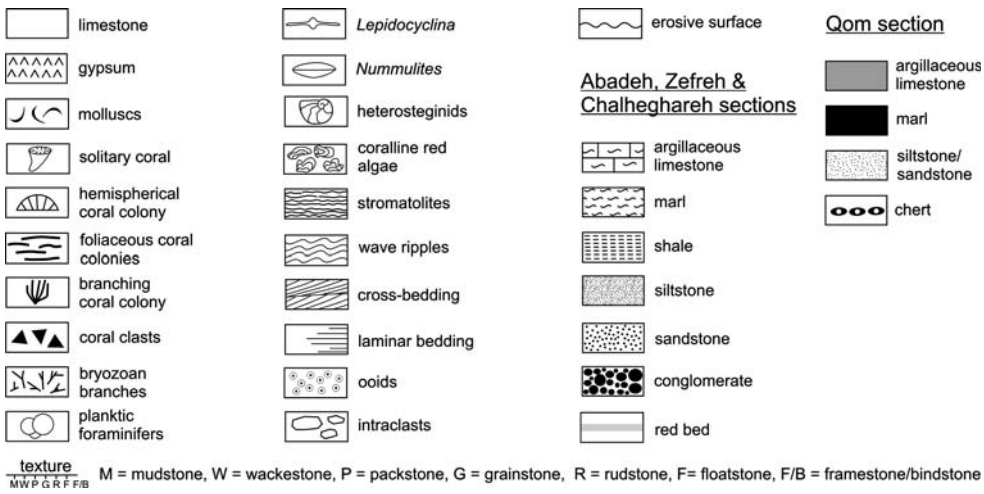

Fig. 4 continued

praebulloides, *Gg. ciperoensis*, *Gg.* ex gr. *brevis*, *Globorotaloides testarugosus*, *Cassigerinella chipolensis*, *Tenuitella munda*, *T. insolita*, and *Tenuitellinata angustiumbilicata*. The coral horizon is topped by gray-green calcareous marls and argillaceous limestones with abundant branching bryozoans in the first meter (21–24).

A prominent, 2.3 m thick bed of calcareous sandstone, covering the marl/argillaceous limestone succession, exhibits *Callianassa* burrows at its top that are filled with *Nummulites* tests (25). The above following argillaceous limestones show intercalations of fine-grained sandstones and frequently contain plant debris and *Nummulites sublaevigatus* (26–27). From bed 28 onwards, argillaceous limestones and marls occur, which include scattered but in situ, dome-shaped, colonial corals with diameters of up to 0.2 m (*Porites*-Faviidae assemblage sensu Schuster and Wielandt 1999) (28). The frequency and size of corals (poritids, faviids) increases upsection and finally form a succession of small patch reefs with lateral extensions of 30–40 m and maximum heights of 5–6 m (29–32). They are dominated by large (max. 1.8 m length, 1 m height), hemispherical coral heads (*Porites*, *Favites*, *Diploastrea*), with minor contributions of thick branching (branch diameter up to 8 cm) corals (*Porites*, *Caulastrea*). Some *Porites* colonies form microatolls (Fig. 5b). Associated with the patch reefs are larger foraminifers [*L.* (*E.*) *dilatata*, *L. undulata*, *L.* cf. *marginata, Rotalia viennoti*, *Heterostegina* cf. *praecursor*, *Operculina complanata*, *Borelis pygmaea*, *Austrotrillina* cf. *striata*, *Archaias* sp.] and gastropods (characteristic are giant strombids and *Diastoma*, see Harzhauser 2004). Together with all other macrofossils, corals disappear in beds 33–34. However, miliolid foraminifers become abundant in the prevailing marls (33–34).

A polymictic conglomerate with an erosional base tops the coral bearing succession (35). It is only locally exposed and composed of well-rounded boulders up to 25 cm length. Laterally the conglomerate disappears and an erosional surface terminates the patch reef-unit. It is covered by gray, green and brown marls, as well as by fine-grained calcareous sandstones with intercalations of coarse-grained sandstones and fine-grained conglomerates (36–40). This part of the section is rich in mollusks. Intercalated is a low-diversity, small-sized potamidid fauna accompanied by abundant cerithids and small neritids (38) (Fig. 10a; Harzhauser 2004). It is overlain by a highly diverse mollusk coquina (41) with various bivalves (*Kuphus melitensis*, giant subrhomboidal lucinids, and *Acropaia emiliae*) and gastropods (giant strombids, archaeogastropods, and thick shelled *Ampullinopsis*) (Mandic 2000; Harzhauser 2004).

Upsection, the siliciclastic content decreases and nodular bioclastic limestones (packstones and floatstones) with corallinaceans, foraminifers, mollusks, and bryozoans occur, which show a thinning upward trend (42–43). Some beds contain soritid and peneroplid foraminifers. Above follows a marl unit with mass occurrence of lepidocyclinids (44; Fig. 5a), and argillaceous limestones (45–48) that are topped by a 200 m wide and up to 16 m thick succession of reefoidal limestones. The reef frameworks are constructed by platy and dome-shaped corals, which are encrusted by coralline red algae (*Neogoniolithon*, *Spongites*) (49–52). The reef succession is overlain by a package of marls containing larger foraminifers (lepidocyclinids, *Rotalia viennoti*, *Amphistegina*, heterosteginids, operculinids), delicate branching bryozoans, and articulated pectinids (*Amussiopecten labadyei*; 53–54) (Fig. 10e). A well-bedded succession follows, comprising corallinacean (*Neogoniolithon*) pack-, float-, grain- and rudstones with *Borelis* cf. *pygmaea*, *Austrotrillina* sp., *Gypsina squamiformis*, amphisteginids, lepidocyclinids, soritids, peneroplids, and heterosteginids (55–58). These bioclastic limestones also include coral communities that show a distinct succession. In the basal part, in situ, non-framework forming coral communities composed of dome-shaped

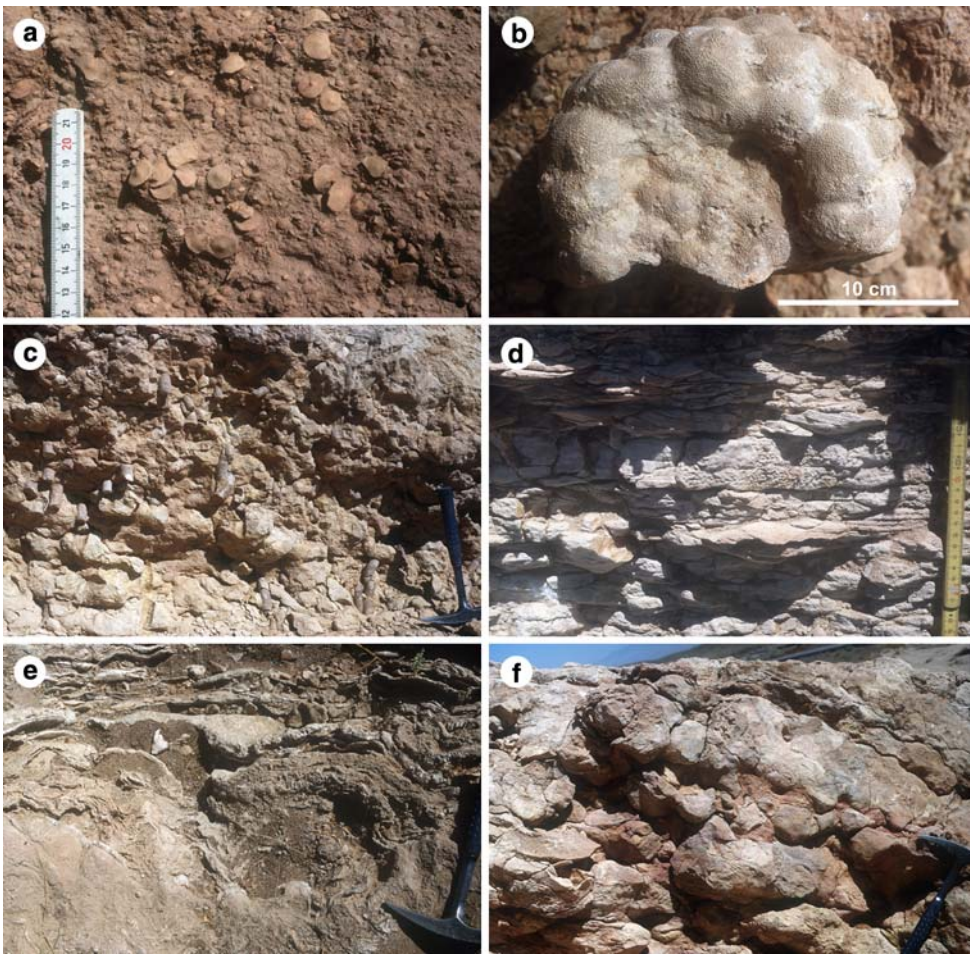

Fig. 5 Lithological aspects of the Qom Formation. **a** Marl with lepidocyclinids from section Abadeh (*44*). The relatively small size of lepidocyclinid tests indicates a relatively shallow water environment. **b** Massive colony of a *Porites* coral from the *Porites*-Faviidae assemblage from Abadeh section (*31*). The developed microatoll documents that the coral grew near the sea-surface and was exposed at lowest tides. **c** Dense in situ population of the teredinid bivalve *Kuphus melitensis*. F-Member of section Chalheghareh (*102*); hammer for scale. **d** Sandstone with oscillation ripples and trough cross-bedding from the d-Member in the Qom section (*34*). **e** Laminated gypsum of the Qom section (*37*); hammer for scale. **f** Paleokarst cavities filled with red continental siliciclastics of the Upper Red Formation. Top of the f-Member limestones at section Chalheghareh; hammer for scale

colonies occur. Upsection these communities are replaced by a bed of framework forming, massive, dome-shaped corals (58), succeeded by grain- and rudstones with toppled and fragmented corals, coralline algal crusts (*Neogoniolithon*, *Spongites*, *Sporolithon*, *Lithoporella*) and rhodolites (*Sporolithon*, *Lithothamnion*) (Fig. 10c; 59–61). Frequent gastropod casts are related to *Cassis*, *Ampullinopsis* and *Globolaria* (Harzhauser 2004).

Zefreh section

Zefreh section is a composite of two section tracts with Zefreh A (Fig. 6) covering the lower and Zefreh B (Fig. 7) the upper segment of the complete section. In Zefreh A (Fig. 6) shallow marine deposits of the Qom Fm. unconformably rest on continental siliciclastics (red conglomerates and green or yellow siltstones) of the Lower Red Fm. (1–3).

The Qom Fm. starts with a unit of predominantly green and brown marls (4–11). At its base interbeds of cross-bedded sandstones and siltstones occur (6, 9, 10). The marls contain a rich fauna dominated by bivalves (e.g., large oysters, *Amussiopecten labadyei*, *A. subpleuronectes*) and gastropods (mainly turritellids and strombids) that are often enriched within coquinas, and a planktic foraminiferal assemblage including *Globigerina* cf. *ciperoensis*, *Globoturborotalia woodi*, *Globigerinoides trilobus*, *Gs. immaturus*, *Gs. quadrilobatus*, *Globigerinella obesa*, *Globoquadrina* cf. *dehiscens*, and *Paragloborotalia* cf. *semivera*.

Upsection follows a unit of limestones (rud- and grainstones with bryozoans), and partly laminated siltstones (12–14). It is topped by a marl succession with abundant mollusks, which is, in turn, terminated by a bed of large oysters (20).

Above follow conglomeratic sandstones and conglomerates (21–23). These grade into a succession of siliciclastics and marls that show a vertical change in color from red to green (24–29). Intercalated are thin layers of bright-green volcanic ashes. The fauna is characterized by mollusks (turritellids, strombids, oysters) while in the upper part branching bryozoans become abundant (26). Pectinid bivalves (*Amussiopecten labadyei*, *A. subpleuronectes*) are present as well. Foraminifers are represented by lepidocyclinids [*Lepidocyclina* (*Eulepidina*) *dilatata*, *L.* (*E.*) aff. *favosa*, *L.* (*Nephrolepidina*) of *morgani*-type],

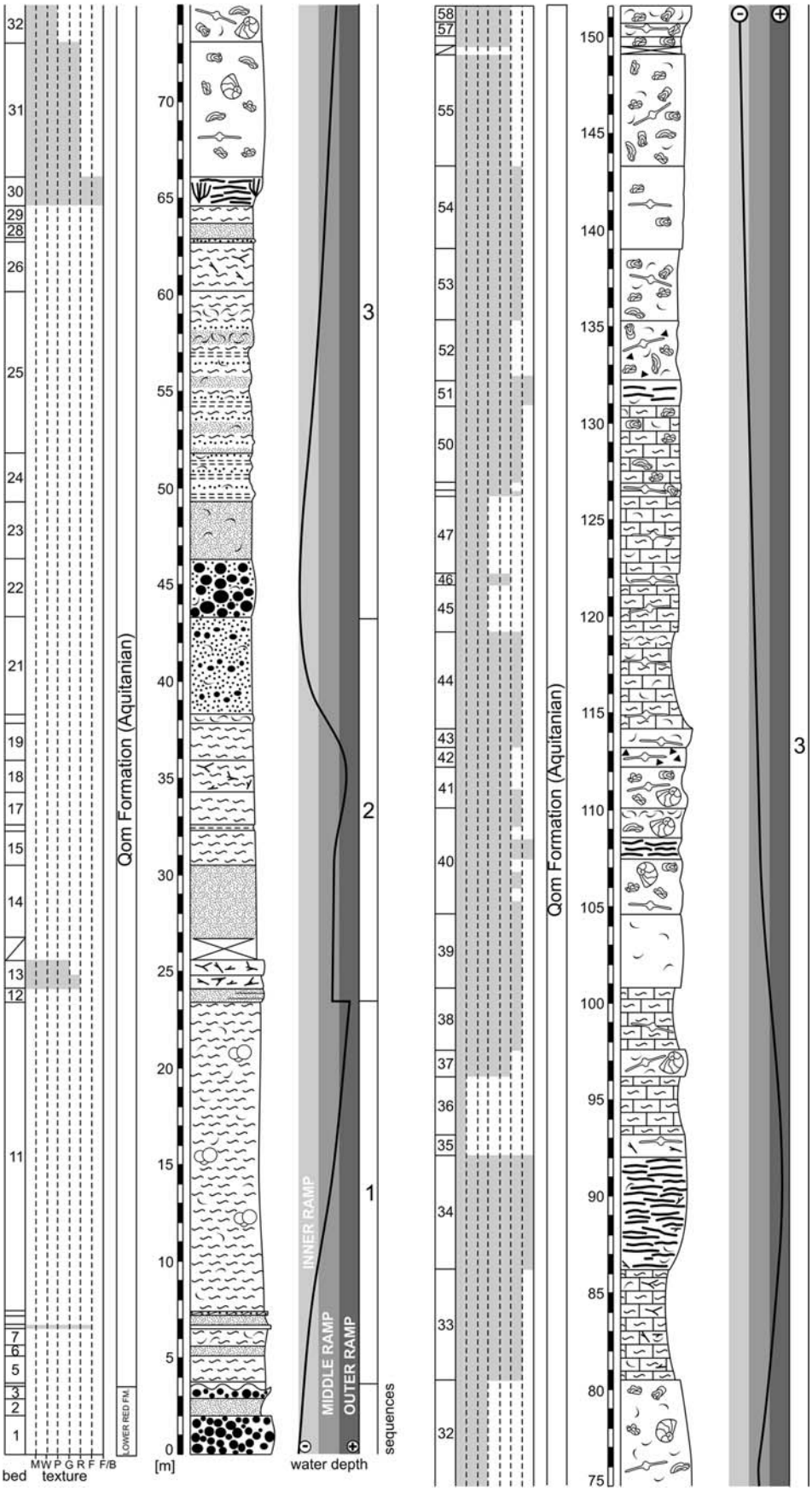

Fig. 6 Zefreh A section; lithological succession, texture, water depth trend and chronostratigraphy; see Fig. 4 for legend

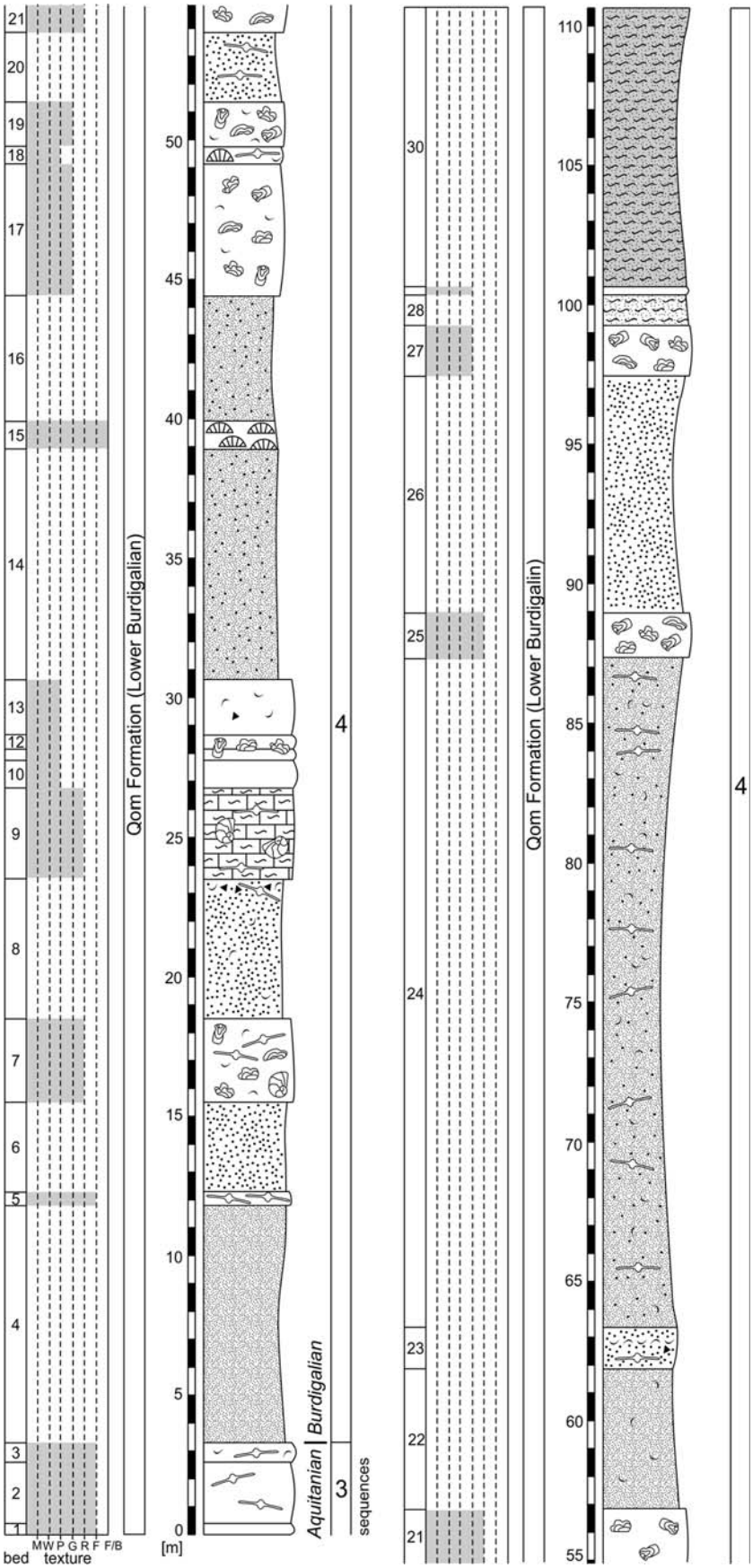

Fig. 7 Zefreh B section; lithological succession, texture, water depth trend and chronostratigraphy; see Fig. 4 for legend

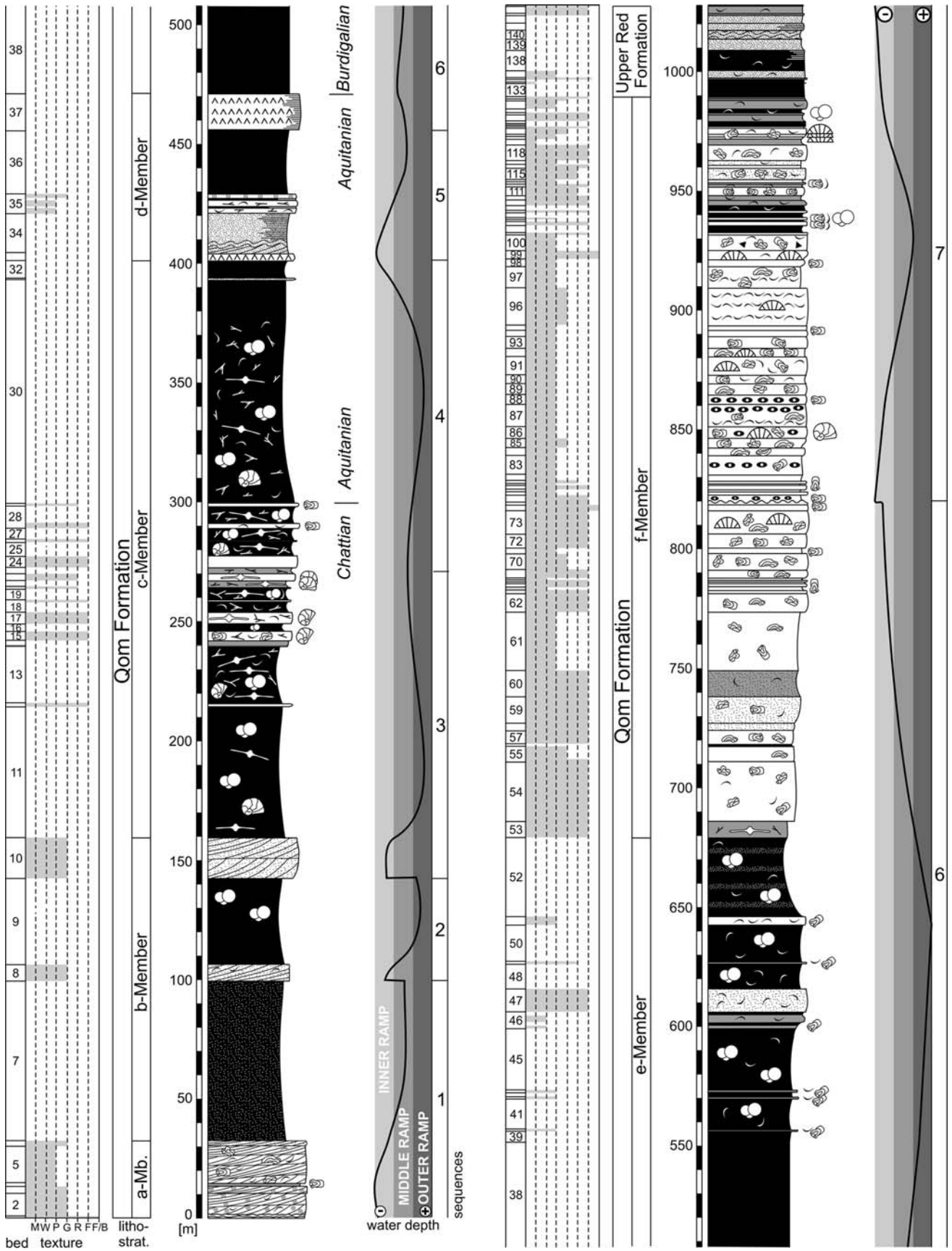
bed
texture
M W P G R F F/B
litho-strat.
Qom Formation
a-Mb.
b-Member
c-Member
d-Member
[m]
Burdigalian
Aquitanian
Chattian
Aquitanian
INNER RAMP
MIDDLE RAMP
OUTER RAMP
water depth
sequences
Upper Red Formation
Qom Formation
e-Member
f-Member

◄ **Fig. 8** Qom section; lithological succession, texture, water depth trend, litho- and chronostratigraphy. Members refer to the lithostratigraphic scheme of Furrer and Soder (1955); see Fig. 4 for legend

Operculina complanata, heterosteginids, and few miogypsinids. Besides, sirenian bones occur sporadically. The marl at its top is intercalated with beds of sandstone and siltstone (27, 28). A coral build-up constructed mainly by *Tarbellastraea* with thickly branching colonies and *Porites* with thick platy growth forms follows above (30). It is capped by a package of skeletal limestones (31, 32) composed of corallinaceans and larger benthic foraminifers (lepidocyclinids, heterosteginids, *Operculina*). A unit of argillaceous limestones with abundant bryozoans follows (33), topped by a coral build-up constructed by *Leptoseris* and *Porites* with platy growth forms (34). The marly interstitial sediment contains abundant bryozoans and lepidocyclinids with large discoid tests. A thick package of carbonates forms the upper part of the Zefreh A section (35–58) with bioclastic floatstones prevailing. Interbedded are bioclastic pack- and rudstones. At the base of this depositional unit, argillaceous limestones with large discoid lepidocyclinids occur (36–38). Upsection the amount of fine-grained matrix decreases. The fauna is here represented by foraminifers (lepidocyclinids, miogypsinids, heterosteginids, *Operculina*, *Amphistegina*, *Austrotrillina*, *Borelis*, *Elphidium ortenburgense*, *E. matzenense*), bivalves (e.g., pectinids, oysters), abundant corallinaceans, as well as gastropods, echinoids, and bryozoans. Some beds contain coral rubble (42, 52) or in situ corals (platy *Porites*; 51, 40). The topmost layers of the carbonatic unit (58) contain *Kuphus* tubes in growth position (Fig. 5d) and articulated pectinids (*Amussiopecten* cf. *subpleuronectes*).

The sedimentary succession continues in section Zefreh B (Fig. 7). Its lowermost three beds are composed of lepidocyclinid floatstones (1–3). These beds are widely traceable and allow a correlation with Zefreh A section. The succeeding part of the section is dominated by terrigenous sandstones and siltstones, while limestone beds occur rather intermittently. Occasionally, coral debris composed of branching *Porites* (8) as well as small *Porites* patch reefs (15) are intercalated in the terrigenous deposits. The limestone beds have a distinct reddish color, contain varying amounts of terrigenous material, and are predominantly composed of corallinacean algae. Occasionally, pectinid bivalves (*Costellamussiopecten pasini*, *Oopecten*), *Clypeaster* echinoids, and larger foraminifers (lepidocyclinids, miogypsinids, *Heterostegina*) significantly contribute to carbonate production. Some beds (1, 17) contain *Kuphus* tubes. The top comprises a succession of silty marls (28–30). Within their lower part is a bed of miliolid grainstone intercalated (29). Above this limestone, the color of the silty marls shifts from gray to red and the Qom Fm. deposits gradually shift into the continental redbeds of the Upper Red Formation.

Qom section

At Qom section (Fig. 8) the underlying Lower Red Fm. consists of red and green claystones. The onset of the Qom Fm. is marked by oolithic grainstones and packstones (a-Member: 1–6). Bioclasts derived from coralline red algae (*Lithothamnion*), echinoids, oysters and other bivalves. Typical is a meter-scaled cross-bedding with intercalated biolaminites showing wavy lamination at mm- and cm-scale (1). Upsection follows a lithostratigraphic unit with silty claystones and marls (b-Member: 7–10). Two intercalated packages with cross-bedded, sandy grainstones (8, 10) contain intraclasts (limestone pebbles, clay pebbles, black pebbles) and glauconite. Scattered shells of *Amussiopecten labadyei* (8) and *Pecten tietzei* (10) are represented therein. Foraminiferal assemblages from the marl below the upper grainstone package (9) include various planktic (*Globigerina praebulloides*, *Gg. ciperoensis*, *Gg. labiacrassata*, *Gg. angulioficinalis*, *Gg. ouachitaensis*, *Globigerinella obesa*, *Globigerinoides primordius*, *Paragloborotalia*? *pseudocontinuosa*, *Cassigerinella chipolensis*) and benthic forms (*Textularia*, *Eggerella*, *Vulvulina*, *Reticulophragmium*, *Haplophragmoides*, *Ammonia*, *Lenticulina*, *Percultazonaria*, *Polymorphina*, *Uvigerina*, *Bolivina*, *Orthomorphina*, *Planulina*, *Cibicidoides*, *Hanzawaia*, *Nonion*). Associated nannoplankton contains *Reticulofenestra abisecta*, *R. bisecta*, and *Zygrhablithus bijugatus*.

A thick unit of marl and interbedded limestone beds follows (c-Member: 11–32). This depositional unit can be divided into three subunits. The lower subunit is formed by marls (11). The middle subunit is an alternation of marls and bioclastic limestones (12–29). Limestones mainly comprise corallinacean-foraminiferal floatstones (*Lithothamnion*, *Neogoniolithon*) with echinoids, oysters and bryozoans (Fig. 10d). Sporadically bryozoan-dominated packstones occur (17; Fig. 10f). The interbedded marls contain bryozoans, pectinids (*Pecten tietzei*, *Amussiopecten labadyei*, *A. subpleuronectes*, *Costellamussiopecten suzannae*), sponge spicules and larger foraminifers. The upper subunit is built up by marls (30), in which bryozoans locally become very abundant. In addition, nuculid bivalves, ostracods, benthic (*Textularia*, *Reussella*, *Lobatula*, *Rosalina*, *Cibicidoides*, *Hanzawaia*, *Ammonia*) and planktic (*Globigerina praebulloides*, *Gg.* cf. *ciperoensis*, *Gg. officinalis*, *Gg. ouachitaensis*, *Globigerinella obesa*, *Globorotalita woodi*, *Paragloborotalia*? *pseudocontinuosa*, *Cassigerinella chipolensis*, *Tenuitellinata angustiumbilicata*) foraminifers are very common. All

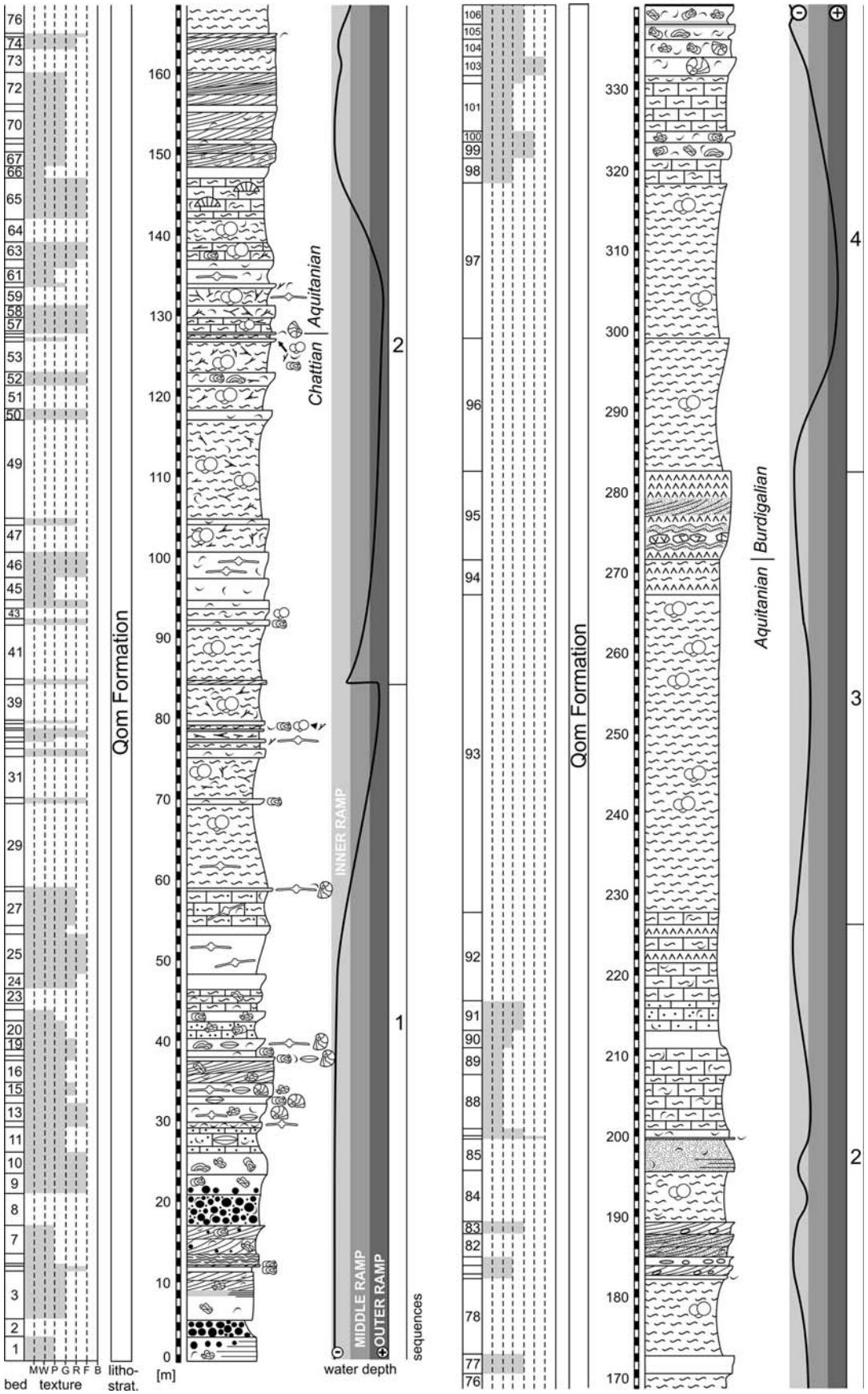
bed
MW P G R F B
texture
litho-strat.
Qom Formation
[m]
Chattian | Aquitanian
INNER RAMP
MIDDLE RAMP
OUTER RAMP
water depth
sequences
Qom Formation
Aquitanian | Burdigalian

◄ **Fig. 9** Chalheghareh section; lithological succession, texture, water depth trend, litho- and chronostratigraphy; see Fig. 4 for legend

subunits of the c-Member exhibit the same larger foraminiferal assemblage. The main contributors are *Operculina* (*O. complanata*, *O.* sp.), heterosteginids [*Heterostegina* (*Vlerkina*) *assilinoides*, *H.* cf. *pusillumbonata*, *Planostegina* aff. *giganteoformis*], *Amphistegina* cf. *lessonii*, and *Lepidocyclina* (*Eulepidina*) *dilatata*. Smaller nephrolepidinids (of *morgani*-type) are less frequent. Additionally, miogypsinids were detected in the middle subunit.

Above, a siliciclastic-dominated unit occurs, made up of marls, sandstones, silts, gypsum and carbonates (d-Member: 33–37). The lower gypsum bed (33) is partly banded and contains gypsum nodules of 0.5 cm in diameter. Red and green siltstones cover the gypsum (34), showing wave ripples and bioturbations at their base, while the upper part exhibits a fine lamination. The siltstones are overlain by ooid grainstones and a series of bryozoan packstones, composed of cm-sized fragments of mostly erect foliaceous, framework-forming bryozoan colonies (35). The bryozoans are accompanied by oysters, pectinids and irregular echinoids. Higher in the section green marls (36) and a package of laminated gypsum appear (37; Fig. 5e).

The gypsum is covered by green and gray marls (e-Member: 38–52) with ostracods and a rich foraminiferal fauna including benthic and planktic forms. *Textularia*, *Spirorutilis*, *Baggina*, *Siphotextularia*, *Heterolepa*, and *Fontbotia* are characteristic benthic foraminifers at the base of the e-Member (38), while benthic foraminifers dominated by *Cibicidoides*, *Uvigerina*, and *Heterolepa* together with *Textularia*, *Spirorutilus*, *Cylindroclavulina*, *Pullenia*, *Melonis*, *Praeglobobulimina*, *Gyroidinoides* occur higher in the e-Member marl sequence (48–52). Planktic foraminifers are represented by *Globigerina ottnangiensis*, *Gg. lentiana*, *Gg.* cf. *ciperoensis*, *Gg.* cf. *officinalis*, *Globigerinella obesa*, *Globigerinoides ruber*, *Gs. quadrilobatus*, *Gs. primordius*, *Gs. trilobus*, *Globigerinella obesa*, *Globorotalia woodi*, *Paragloborotalia*? *inaequiconica*, *Paragloborotalia*? *pseudocontinuosa*, *Globorotaloides suteri*, and *Cassigerinella chipolensis*. The nannoplankton flora consists of *Reticulofenestra abisecta*, *R. floridana*, *Sphenolithus moriformis*, *S.* cf. *umbrellus*, *S.* cf. *pseudoradians*, *Helicosphaera bramletti*, *H.* cf. *intermedia*, *H.* cf. *compacta*, *H.* cf. *carteri*, *Coccolithus pelagicus*, *C.* cf. *micropelagicus*, *Coronocyclus* cf. *nitescens*, and *Pontosphaera* sp. Ostracods and burrowing echinoids (*Schizaster*, 51) are also common. Some layers are strongly bioturbated, others contain a high amount of terrigenous quartz (52). Float- and packstone intercalations contain echinoids, rhodolites, and mollusks (Harzhauser 2004). Conspicuous are monospecific coquinas with articulated shells of the pectinid bivalve *Costellamussiopecten pasini* (44–51).

The e-Member marls grade into a carbonate package (f-Member: 53–132), which can be subdivided into three subunits. In the lower one (53–75), marls are still intercalated between bioclastic corallinacean-echinoderm floatstones with dominating *Lithothamnion*, *Neogoniolithon*, and *Spongites* among corallinaceans. At the top of this subunit isolated *Porites* corals with massive hemispherical growth forms occur in situ (73). The lower subunit is terminated by an erosional surface.

The middle part of the f-Member (76–101) is mainly composed of packstones. Some beds contain accumulations of mollusks, larger foraminifers, echinoids (*Clypeaster*, in 89 and 101) or isolated colonial corals (*Porites*). In bed 96 corals are associated with the thick-shelled bivalves *Gigantopecten holgeri*, *Modiolus escheri*, *Periglypta miocaenica*, and *Megacardita crassa taurovata*. Chert concretions are enriched in some layers (76, 83, 88–87).

Upsection follows a subunit with a higher pelitic content (102–132), including marls and corallinacean limestones (floatstone, rudstone, packstone, grainstone). In marly interbeds (102–108) benthic foraminifers (*Ammonia*, nonionids) are common, while planktic foraminifers (*Globigerina praebulloides*, *Gg. postcretacea*, *Gg. dubia*, *Gg. lentiana*, *Gg. ottnangiensis*, *Cassigerinella chipolensis*, *C. boudecensis*, *Turborotalia quinqueloba*, *Tenuitella*? *brevispira*, *Tenuitellinata angustiumbilicata*) rarely occur. Corals (Schuster and Wielandt 1999), bivalves (Mandic 2000), and gastropods (Harzhauser 2004) are abundant. Usually, corals occur as isolated dome-shaped and branching colonies up to 70 cm in diameter and only sporadically form small (3–4 m width, 1.5 m thick) patch reefs constructed mainly by faviids and *Caulastraea* (120–121). The coralline algal flora is relatively diverse and comprises encrusting growth forms as well as rhodolites both of *Spongites, Neogoniolithon*, *Lithothamnion*, *Sporolithon*, and *Lithoporella* species. The patch reefs interfinger with grain- to packstones with a typical miliolid-soritid-*Borelis* foraminiferal assemblage (Fig. 10b), comprising *Borelis melo curdica*, *B. melo melo*, *B. haueri*, *Dendritina rangi*, *Archaias hensoni*, *A. asmaricus*, *Peneroplis armorica*, *P. laevigatus*, *P. evolutus*, and *Spirolina* sp. The pectinid fauna comprises *Gigantopecten holgeri*, *Amussiopecten expansus*, *Manupecten puymoriae*, and *Pecten subarcutus*.

The transition of the Qom Fm. into the Upper Red Fm. (133–145) is gradual and characterized by a drastic increase of siliciclastics. Fossiliferous [echinoids, gastropods (e.g., *Ficus*, *Strombus*), bivalves (*Gigantopecten holgeri* and *Manupecten puymoriae*)] red marls, siltstones and fine-grained sandstones prevail. Intercalated are monotypic coquinas of the clam *Polymesoda* aff. *brogniarti*. Reddish, fine-grained sandstones with wave ripples, laminated siltstones with plant debris, and conglomerates of the Upper Red Fm. terminate the Qom section.

Chalheghareh section

At section Chalheghareh (Fig. 9), deposits of the Qom Fm. cover reddish continental conglomerates and sandstones with intercalated paleosoils of the Lower Red Fm. The contact is not exposed.

The marine succession of the Qom Fm. starts with conglomerates, cross-bedded, coarse-grained sandstones with small nummulites, rhodolites (*Lithothamnion*), coralinacean debris and fragmented echinoids intercalating with parallel and cross-bedded corallinacean (*Lithothamnion*) packstones, rudstones and grainstones with abundant rotaliid and nummulitid foraminifers, as well as pectinid bivalves (*Pecten tietzei*, *Amussiopecten labadyei*, *Aequipecten submalvinae*) (1–28). Grainstones of bed 3 include a reddish colored zone, and bed 6 is a stromatolithic limestone with wavy mm- to cm-scale lamination. In bed 12 shells of large oysters are accumulated. Upsection (22–28) the coarse siliciclastic content decreases and interbeds of marl and argillaceous limestone with

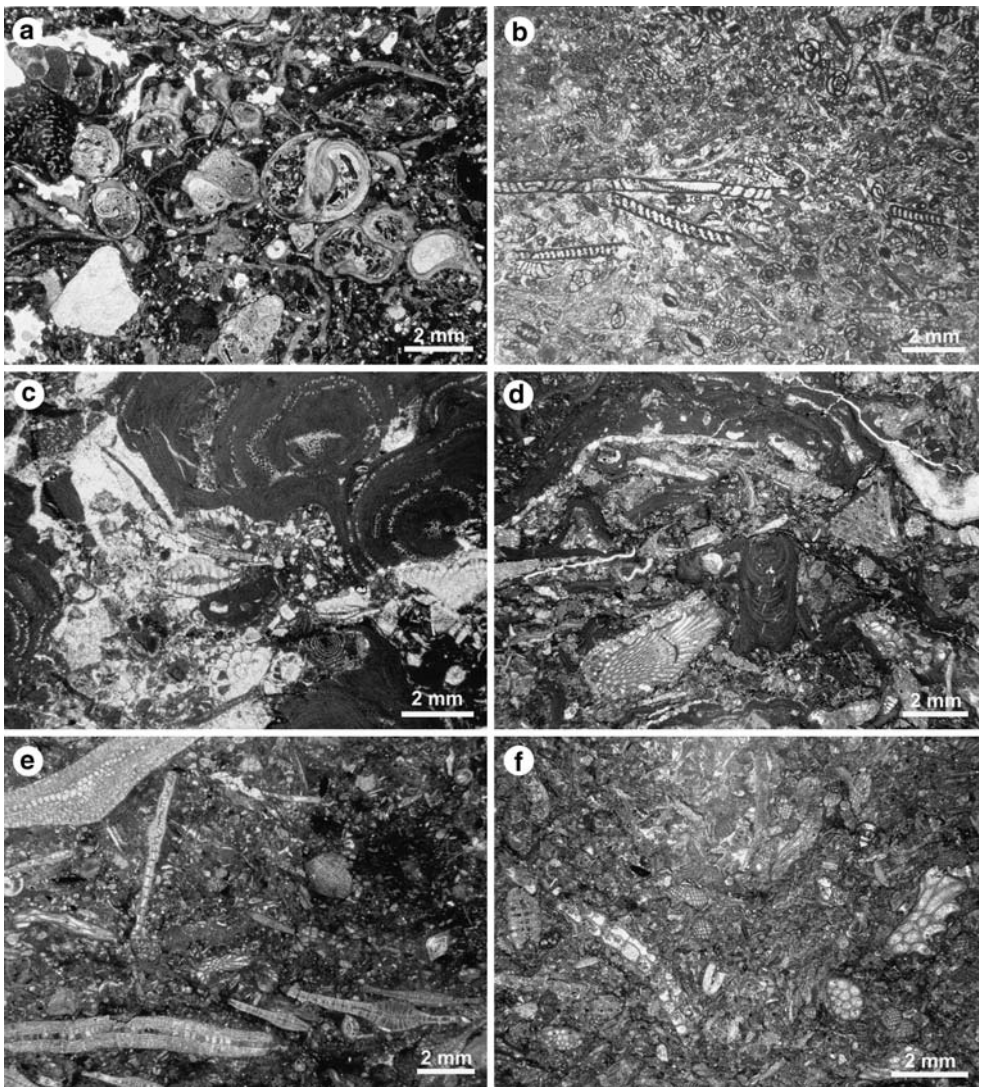

Fig. 10 Thin section microphotographs illustrating the depth zonation of biotic assemblages from Oligo-/Miocene ramps in the Esfahan-Sirjan and Qom basins. **a** Gastropod (potamidids) coquina with a high amount of detritic quartz, lithic grains and coral (*Porites*) clasts indicating a nearshore environment in the vicinity of mangroves (Abadeh 38). **b** Miliolid-grainstone with *Archaias* and *Borelis*. The dominance of porcellaneous foraminifers points to a shallow, restricted inner ramp environment with seagrass vegetation (Qom 15). **c** Foraminiferal-corallinacean rudstone with *Sporolithon*, *Borelis*, heterosteginid and rotaliid foraminifers from a shallow inner ramp setting (Abadeh 61). **d** Corallinacean-bryozoan floatstone of a moderately deep environment on the middle ramp. Bryozoans are represented by erect delicate branching, and unilaminar encrusting growth forms (Qom 18). **e** *Lepidocyclina*-bryozoan floatstone. The large size and flat discoidal shape of *Lepidocyclina* tests is typical for a deep low light environment on the outer ramp. Associated with the lepidocyclinids are erect delicate branching bryozoans (Abadeh 53). **f** Bryozoan-packstone composed of erect delicate branching, erect bilaminar, and erect foliaceous colonies from the outer ramp. This facies represents the deepest environment, where erect bryozoans have the highest abundance and diversity, and where light dependent biota is completely missing (Qom 28)

lepidocyclinids occur. A series of marls with intercalated limestones follows (29–66). The latter are concentrated in the middle segment of this unit (30–48) and comprise *Lepidocyclina* (eulepidinids) floatstones as well as oyster coquinas (*Hyotissa hyotis*) that are accompanied by erect branching and nodular growing bryozoans (36, 38). Bryozoans, mainly of the erect rigid fenestrate growth type, become more frequent in the upper part of the unit. In particular, bed 58 is formed by a bryozoan floatstone that is characterized by a diverse fauna with large fragments of erect growth forms including fenestrate, foliaceous and delicate branching, as well as flexible growth types. Associated planktic foraminifers belong to *Globigerinoides primodius*, *Gs. immaturus*, *Gs. quadrilobatus*, *Globigerina praebulloides*, *Gg.* cf. *ottnangiensis*, *Globigerinella obesa*, *Cassigerinella boudecensis*, *Tenuitella clemenciae*, *Tenuitellinata angustiumbilicata*. *Operculina complanata* and lepidocyclinids [*E. dilatata*, *E.* cf. *formosoides*, *L.* (*N.*) *morgani*-type, *E. undulosa*?, *L.* cf. *elephantina*?] are the most abundant larger foraminifers, while *Heterostegina* (*Vlkerkina*) *assilinoides* and *Amphistegina* are frequent. Additionally, miogypsinids (*Miogypsinoides formosensis*, *M. bantamensis*) occur above bed 55. Sponge spicules and pectinids are also present. In beds 29–49 the pectinid fauna comprises *Pecten tietzei*, *Amussiopecten labadyei*, *A. subpleuronectes* and *Costellamussiopecten suzannae*, whereas the pectinid fauna in beds 59–63 becomes restricted to *P. tietzei* and *A. subpleuronectes*. A marly floatstone with isolated, in situ, dome-shaped corals (*Porites*, *Goniopora*, bed 65) and rhodolites (*Spongites*, *Lithoporella*, *Lithothamnion*, *Sporolithon*), as well as a bed of wackestone (66) terminate this unit.

Upsection, rippled oolithic and peloidal, bioclastic (echinoids, mollusks, corallinaceans) grainstones (67–72) follow, occasionally containing monospecific potamidid gastropod faunas. These beds are followed by thick marly layers grading into siltstones (73–85) and mollusk-dominated coquinas (86, 87). Intercalated grainstones are often cross-bedded and associated with mud-pebbles. The benthic microfauna of the marls consists of ammonias and pararotalias, and rare sponge spicules (78, 84). Plankton is represented by *Globigerina praebulloides*, *Gg.* cf. *ciperoensis*, *Gg. officinalis*, *Gg. ouachitaensis*, *Globoturborotalita woodi*, *Globigerinoides primordius*, *Cassigerinella boudecensis*, and *Tenuitella munda*. Argillaceous limestones (88–92) containing bivalves (e.g., *Costellamussiopecten pasini*) and echinoids follow above. Here, the benthic foraminiferal fauna is more diversified, yielding *Cibicidoides*, *Hanzawaia*, *Eponides*, *Nonion*, and *Textularia*. In bed 92 thin gypsum crusts are intercalated. The sedimentary succession continues with green marls (93–94) containing agglutinating benthic foraminifers (*Jadammina*, *Ammotium*, *Ammobaculites*) as well as planktic foraminifers (*Globigerina officinalis*?, *Cassigerinella chipolensis*, *C. boudecensis*, *Tenuitella gemma*), and ostracods. Thin gypsum interbeds occur at the top of the marls (94), grading into a thick evaporite unit (95). Its base consists of thin (<5 mm) gypsum layers with oscillation ripples that alternate with cross-bedded, fine-grained, reddish siliciclastics. Upsection the siliciclastic intercalations become thinner and finally disappear. A single bed contains large gypsum clasts (Ø 40 cm). The evaporites are covered by green marls (96–97), which are devoid of benthos while plankton is present.

The uppermost unit of section Chalheghareh is formed by fossiliferous limestones (grainstone, packstone, rudstone; 98–106) composed of peloids, mollusks, echinoderms, corallinaceans and foraminifers (*Operculina*, *Austrotrillina*, few soritids, miogypsinids). They further contain rhodolites, gastropods and infaunal bivalves. Some beds are characterized by mass occurrences of the irregular echinoid *Parascutella* (104, 105) and the teredinid bivalve *Kuphus melitensis* in life position (Fig. 5c). Moreover, *Kuphus* coquinas occur (103, 105), which can be traced for hundreds of meters (in another section located about 8 km in WNW direction similar *Kuphus* layers appear in the same stratigraphic position). The top surface of bed 105 has a reddish color and the top of the limestone succession shows karst fissures infilled with violet siltstone (Fig. 5f). It is assumed that it represents the boundary to the above following Upper Red Fm.

Sedimentary evolution of the Qom formation

Depositional environments in the Esfahan-Sirjan fore-arc basin

Abadeh section

Section Abadeh includes three depositional sequences (Fig. 4). Terrestrial sediments of the Lower Red Fm. are deposited during the lowstand of the first sequence. Flooding of the platform is indicated by nummulitic siliciclastics deposited in a nearshore environment. With increasing water depth, the coarse siliciclastic content decreases and pure siliciclastics become substituted by argillaceous limestones and marls, for which offshore conditions are indicated by plankton assemblages (1–5). A deeper offshore environment with reduced light levels is also suggested by Schuster and Wielandt (1999) for the associated solitary coral assemblage.

A subsequent sea-level drop is indicated by an alternation of marls with thin interbeds of sandstones (6–15) that may represent a lowstand fan terminating the first

sequence. Paleoecological interpretations of the *Turritella*-dominated gastropod fauna suggest a shallow to moderately deep sublittoral environment for this part of the section (Harzhauser 2004). The upsection loss of sand, and the solitary coral assemblage in marls with abundant plankton, documents a new rise of relative sea-level during the second depositional sequence. Associated erect branching bryozoans suggest low water energy conditions in a deeper habitat (e.g., Smith 1995), as is also indicated by the co-occurring lepidocyclinids, which are represented by large discoid forms that are typical for deeper, low light environments (Hallock 1985; Hallock and Glenn 1986; Pedley 1998). Accompanying *Leptoseris* build-ups (20) also point to a relatively deep environment (Kahng and Maragos 2006). Argillaceous limestones with sandy intercalations (23–27) preluded a shallowing succession. *Nummulites* tests in *Callianassa* burrows of bed 25 point to relocation and represent relictic, storm generated deposits that are trapped in the burrows (Wanless et al. 1988; Beavington-Penny et al. 2006). Sustained shallowing is documented by the coral-bearing succession above (28–32). The presence of sparsely distributed, large, hemispherical colonial corals in life position (Perrin et al. 1995), and the high content of clay in limestones, indicate a moderately deep environment below the fair-weather wave base. Upsection, colony size and frequency of corals increase and the non-constructional coral assemblage shifts into a patch reef facies for which Schuster and Wielandt (1999) discuss a water depth between 5 and 20 m. Microatolls on some coral colonies (Fig. 5b) document that vertical reef growth was limited by the sea-surface, and that corals on top of the patch reefs became exposed at lowest tides (Woodroffe and Gagan 2000). The gastropod fauna from the inter-reef areas is characterized by herbivorous taxa pointing to the presence of seagrasses (Harzhauser 2004). Upsection the shallowing trend continued and a restricted lagoonal milieu established, as indicated by the dominance of porcellaneous foraminifers (Sen Gupta 1999) in the marl on top of the patch reef facies (34). The second sequence terminates with an erosional surface that reflects emersion.

The third sequence is initiated by a fluvial conglomerate (35) that was deposited during a sea-level lowstand and which is followed by a thin succession of coastal clastics. The latter contain intercalated, low-diversity, potamidid-neritid gastropod coquinas (Fig. 10a) that suggest a littoral environment with fluctuating salinities in the vicinity of mangroves (Harzhauser 2004). Highly diverse mollusk faunas from the overlying bioturbated marls (41–48) point to a shallow subtidal and restricted lagoonal environment with seagrass meadows (Mandic 2000; Harzhauser 2004). The associated benthic foraminiferal fauna supports the assumption of seagrass with the occurrence of soritids and peneroplids (Sen Gupta 1999). A coral reef sequence follows above (49–52), which indicates a minimal rise of relative sea-level that provided the necessary accommodation space. The reef facies is formed by massive hemispherical and crustose corals as well as by coralline red algae that form a rigid framework with a high resistance against wave damage in a shallow exposed position. The large discoid tests of lepidocyclinids, abundant delicate branching bryozoans, planktic foraminifers, and articulated pectinids in marls above the reef limestone (53–54; Fig. 10e) point to a low energy, turbid and low light environment (Hallock 1985; Hallock and Glenn 1986). It established during maximum flooding after drowning of the reef.

The thick package of skeletal limestones above (55–61) is mainly composed of remains of light-dependent biota (corallinaceans, larger foraminifers, corals). It therefore suggests a formation in the shallower photic zone during a relative sea-level fall. At the base of the skeletal limestone succession floatstones dominate. These were deposited in relatively deep settings below the fair-weather wave base, as indicated by their high content of fine-grained matrix. Upsection, increasing fragmentation of the bioclasts caused by an increase in water energy, and loss of matrix due to winnowing is noticed. The corallinacean-foraminiferal rud- and grainstones (Fig. 10c) are indicative of a shallow subtidal setting. Because the density in coral cover decreases with depth (Perrin et al. 1995), the shift from an in situ, non-constructional coral community with large hemispherical colonies (55–57) to an in situ patch reef assemblage (58) displays shallowing. The limestones above the patch reef facies suggest an increase in water energy and shallowing since they exclusively contain toppled coral colonies and coral rubble. Abundant soritids and peneroplids point to seagrass meadows (Sen Gupta 1999).

Zefreh sections

In the Zefreh sections (Figs. 5, 6) four depositional sequences (Zefreh A: three sequences, Zefreh B: one sequence) are recognized in the Qom Fm., which transgrade over continental siliciclastics of the Lower Red Fm. (A1–3). The beginning of the first sequence is a thin alternation of marl and siliciclastics (A4–10) with a marine fauna for which a shallow nearshore environment is indicated by cross-bedding texture. Subsequently, marls developed (A11) for which abundant plankton indicates increasing water depths and a deeper offshore environment.

A package of bryozoan rud- and grainstones (A13), and siltstones (A12, 14) initiate the onset of the second sequence. For their formation, the high amount of terrigenous quartz and the rudstone texture suggest a shallow

environment after a relative sea-level drop. The preferred habitat of most erect, rigid, branching bryozoans is generally a calm milieu below the storm wave base (e.g., Smith 1995), but with shallowing they may have become reworked and accumulated in shallower water. The marls above (A15–19) document a renewed deepening.

Sandstones and coarse-grained conglomerates from above the marls (A21–23) indicate a relative sea-level lowstand and mark the beginning of the third sequence. With ongoing deepening the coarse siliciclastic content decreases upsection and the lithology shifts into an alternation of silt, silty marls and clays (A24–29). The associated mollusk fauna (Harzhauser 2004) and sirenian bones imply seagrass vegetation in a shallow environment. A shallow and turbid environment is also reflected by the *Porites-Tarbellastraea* assemblage in bed A30. The prevailing platy and branching coral growth forms are inferred to be adaptations to a high influx of fine siliciclastic material (Wilson and Lokier 2002; Rosen et al. 2002). With rising relative sea-level the siliciclastic input decreases and skeletal limestones composed of corallinaceans and larger foraminifers (A31–32) were formed, which are typical for the middle ramp. Above follows a unit of bryozoan rich marl (A33), again suggesting deposition in a relatively deep environment. *Leptoseris*-dominated coral build-ups (A34), which are indicative of low light levels in a deeper environment (Kahng and Maragos 2006), mark the maximum flooding of the third sequence. The upsection decrease of clay as well as the high proportion of light-dependent biota (corallinaceans, larger foraminifers, corals) in the carbonatic unit on top of section Zefreh A document a fall in sea-level. The associated coral fauna is characterized by *Porites* with platy growth morphologies, which typically occur in turbid, low light settings with a high input of fine siliciclastics (Wilson and Lokier 2002). This scenario is supported by the high amount of matrix in the framing skeletal limestones.

The upper part of Zefreh section (Zefreh B) belongs to a new sedimentary cycle. Strong siliciclastic influx from the volcanic arc now prevails while the formation of skeletal limestones, containing terrigenous clasts and showing a reddish color, occurs rather sporadically. The strong input of siliciclastics indicates uplift of the volcanic arc that superimposed the eustatic sea-level signal. Therefore, shallow marine conditions of an inner to mid-ramp environment continuously prevailed during deposition of the siliciclastics and limestones above (B4–30). This is supported by the omnipresence of light-dependent biota and absence of deeper water faunal elements, such as planktic foraminifers, abundant erect bryozoans, and *Leptoseris* corals. Indicator for a turbid, relatively nutrient-rich environment is the monotypic *Porites* assemblage in beds B15 and B18 (Wilson and Lokier 2002). The upper part of the section documents siltation as suggested by the shift from gray to red silty marls that grade into continental siliciclastics of the Upper Red Fm. (B28–30). An intercalated bed of miliolid grainstone (B29) implies a shallow restricted environment of an inner shelf lagoon (Sen Gupta 1999).

Depositional environments in the Qom back-arc basin

Qom section

Section Qom includes seven depositional sequences. The first sequence starts with biolaminites and large scale cross-bedded, oolithic, skeletal grainstones (2–3, 5–6) of the a-Member. They are interpreted as subaquatic dunes that formed in the peritidal and shallow subtidal zone and that were deposited during a relative sea-level lowstand.

The a-Member deposits are covered by mudstones of the b-Member, implying a deeper and calm offshore milieu owing to the occurrence of abundant plankton. However, the two intercalated packages of cross-bedded grainstones (8, 10), also interpreted as subaquatic dunes, indicate short episodes with recurrence of shallow subtidal conditions and are assumed to represent lowstand deposits of a second and a third sequence. For the third sequence, the marl succession of the lower subunit of the c-Member (11), the muddy substrate, and the abundant occurrence of plankton and erect branching bryozoans suggest a deeper offshore and relatively low energy environment that evolved during a new rise of relative sea-level. Yet the associated larger foraminifers document deposition to have taken place in the photic zone even at this stage. The corallinacean-bryozoan facies of the marl/limestone succession of the middle subunit (12–29; Fig. 10d) is indicative for sediment export from a moderately deep environment during relative sea-level lowstand of the fourth sequence.

A new drop of relative sea-level is indicated by a bed of cross-bedded sandstone (31) and furthermore by a general increase of terrigenous material. A unit of gypsum in the basal d-Member (33) documents hypersaline conditions during relative sea-level lowstand, initiating the fifth sequence. In the Qom section, rippled sandstones and siltstones on top of the gypsum (34, Fig. 5d) are indicative of a very shallow environment. Upsection these sand- and siltstones are laminated, suggesting an increasing water depth, and grade into a unit of marls (35–36), for which the associated fauna implies fully marine conditions. Bryozoan floatstone interbeds at the base of the marl unit (35) indicate a relatively deep environment, whereas the ooids, forming a succeeding bed, are interpreted to having been reworked from a shallow source area.

Thick gypsum deposits (37; Fig. 5e) reflect a relative sea-level fall and restriction of the basin during lowstand at

the beginning of the sixth sequence (top of d-Member). Foraminiferal fauna and bioturbation in marls above the gypsum (e-Member) documents reconstitution of fully marine conditions with rising relative sea-level. The succession of benthic foraminiferal assemblages from the e-Member marls (substitution of a shallow *Textularia–Spirorutilus–Baggina–Fontbotia* assemblage by a deeper *Uvigerina–Cibicidoides–Heterolepa* assemblage) displays the deepening trend. In contrast, the overlying bioclastic limestone succession of the lower subunit of the f-Member (53–75) developed during the regressional stage of the sixth sequence because of the dominance of light-dependent biota. Corals are restricted to the uppermost part of the sixth sequence (73) during which a suitable shallow water depth was reached. The sixth sequence terminates with an erosional surface that indicates emersion (base of bed 76) and is interpreted as a sequence boundary.

The middle subunit of the f-Member includes the low- and highstand deposits of a seventh sequence. With rising water depth corallinacean limestones (76–101) developed in a shallow to moderately deep environment as indicated by the associated coral faunas. The above following marl interbeds with plankton (102–108) indicate continued deepening.

A new shallowing trend is reflected by the corallinacean limestone package in the upper subunit of the f-Member (109–123). Fragmentation of skeletal grains and the predominantly grain-supported textures point to a turbulent regime during deposition of these beds. Associated patch reefs with *Caulastrea* and faviids also reflect a shallow water depth. Their surrounding sediments are composed of porcellaneous miliolid and soritid foraminifers, which document seagrass vegetation in a shallow, restricted, inner ramp environment (Fig. 10b; Sen Gupta 1999). The transition into the continental Lower Red Fm. is gradual and without hiatus. Obvious is the drastic increase of fine siliciclastic material that interfingers with the bioclastic limestone, which was formed in a low energy, marginal marine environment (Harzhauser 2000) as shown by intercalated coquinas of the marsh clam *Polymesoda* aff. *brogniarti* and an increasing terrigenous influx.

Chalheghareh section

Section Chalheghareh (Fig. 9) contains four depositional sequences. The mixed siliciclastic-carbonate sedimentary succession at the base of the first sequence (1–28) indicates a high-frequency oscillating relative sea-level. Cross-bedded grainstones and siliciclastics with marine biota (1–3, 7–9) refer to the shallow subtidal zone, while an intercalated biolaminite (6) represents the intertidal zone, and a reddish horizon (3) even indicates emersion and pedogenesis. Upsection the decrease in grain size of terrigenous particles, the loss of intertidal deposits, and the increase of marly lithologies with plankton provide evidence for increased water depth. Subsequently, decreasing water depth is represented by intercalations of bioclastic limestones that were exported from a shallower source area, as indicated by the mixture of deeper water (planktic foraminifers, delicate branching bryozoans) and shallower water biota (corals, mollusks, corallinaceans), and the high degree of fragmentation of skeletal grains. One limestone bed documents a high-energy regime due to a large-scale, cross-bedding texture (40) and is therefore suggested to represent the relative sea-level lowstand of sequence two. In the marls above the increase in quantity and diversity of bryozoans, especially of those with erect growth types, suggests an increase in water depth. Bryozoan diversity and frequency is highest in bed 58 and the large size of bryozoan colony fragments points to a more or less in situ deposition. Floatstones with a non-framework forming coral assemblage (65) are assigned to moderately deep environments and imply an environmental change back to shallower conditions.

During step-wise changes in sea-level, a turbulent regime in the shallow subtidal was intermittently installed, as indicated by the presence of cross-bedded (67–75) and oolithic limestones (67–68). These coarser-grained units are intercalated between marls containing planktic foraminifers. Terrigenous material occurring together with black pebbles (79–83), and the first occurrence of evaporites (92) characterize the relative sea-level lowstand at the beginning of sequence three. Marls from above the lower gypsum unit are interpreted to have formed in very shallow conditions due to the occurrence of the benthic *Jadammina–Ammotium–Ammobaculites* assemblage (93), which is typical for coastal marshes (Sen Gupta 1999), although planktic foraminifers are also present, pointing to marine conditions in the central basin. A bed containing gypsum intraclasts in the upper gypsum unit (95) provides evidence for subaerial exposure and reworking of previously precipitated material. The upper gypsum unit is therefore interpreted as lowstand deposit initiating the fourth sequence.

A thick marl unit (96–97) follows above the gypsum, displaying onset of marine conditions by the presence of planktic organisms. The overlying bioclastic limestone succession again displays decreasing water depth. Rhodolites, as well as the grain-supported texture and well sorting, point to a turbulent water regime. Widely traceable *Kuphus*-coquinas (103, 105) are interpreted as tempestites and document deposition above the storm wave base. Karst cavities on top of the bioclastic limestone package are filled with sediments of the Upper Red Fm., documenting emersion and erosion of the Qom Fm. sediments prior to formation of the Upper Red Fm. (Fig. 5f).

Stratigraphy and correlation of the sections

Facies analyses revealed four Upper Oligocene and three Lower Miocene sequences in the fore-arc sections, as well as three Upper Oligocene and three Lower Miocene sequences in the back-arc sections. Within the biostratigraphic framework, the recognized depositional sequences generally correlate well with third order fluctuations of the eustatic sea-level curve of Hardenbol et al. (1998) and allow a basin-spanning correlation of the Qom Fm. (Fig. 11). However, while sequence correlation in the Qom section is reatively well-defined due to its central position in the Qom back-arc basin, the close proximity of the sections Chalheghareh and Zefreh to the volcanic arc makes it likely that vertical tectonic movements overprint the eustatic signal.

Stratigraphic framework of the Esfahan-Sirjan fore-arc basin

In section Abadeh (Fig. 4) the Rupelian/Chattian boundary is pinned down by the first occurrence of lepidocyclinids [*Lepidocyclina* (*Nephrolepidina*) *morgani*-type, *L.* (*Eulepidina*) *formosoides*, *L.* (*E.*) *favosa*] recorded in bed 14 in the lower part of sequence 2 [BouDhager-Fadel and Banner 1999; Cahuzac and Poignant 1997 (SB22b)]. Therefore, sequence 1 is considered to be late Rupelian in age and is, accordingly, correlated with cycle Ru 3 of Hardenbol et al. (1998). The early Chattian age of sequence 2 is corroborated by planktic foraminiferal assemblages, comprising *Paragloborotalia opima opima*, *Globigerina ciperoensis*, *Chiloguembelina*, *Guembelitria*, and *Tenuitella munda* from beds 16–20 (sequence 2), which are referred to zone P21b of Berggren et al. (1995). For the upper part of section Abadeh (above the fluvial conglomerate of sequence 3), pectinid and gastropod faunas also point to a Chattian age (Mandic 2000; Harzhauser 2004). Consequently, sequences 2 and 3 are correlated with cycles Ru 4/Ch 1 and Ch 2, respectively.

In the Zefreh area, Chahida et al. (1977) placed sediments of the Qom Fm. into the Early Miocene (Aquitanian to early Burdigalian) based on the occurrence of *Miogypsina* (*Miogypsinoides) dehaarti.* The section analysed in this study (Fig. 6) also contains *Miogypsina* tests in beds 15–19 (sequence 2). Although their poor preservation does not allow a specific identification, their association with the planktic foraminiferal assemblage of *Globigerina* cf. *ciperoensis*, *Globoturborotalia woodi*, *Globigerinoides trilobus*, *Gs. immaturus*, *Gs. quadrilobatus*, *Globigerinella obesa*, *Globoquadrina* cf. *dehiscens*, and *Paragloborotalia* cf. *semivera* indicates an Early Miocene age (Aquitanian to early Burdigalian) for sequence 2. Furthermore, sequences 1 and 2 contain an *Amussiopecten subpleuronectes-A. labadyei* assemblage, which suggests a late Chattian to early Aquitanian age.

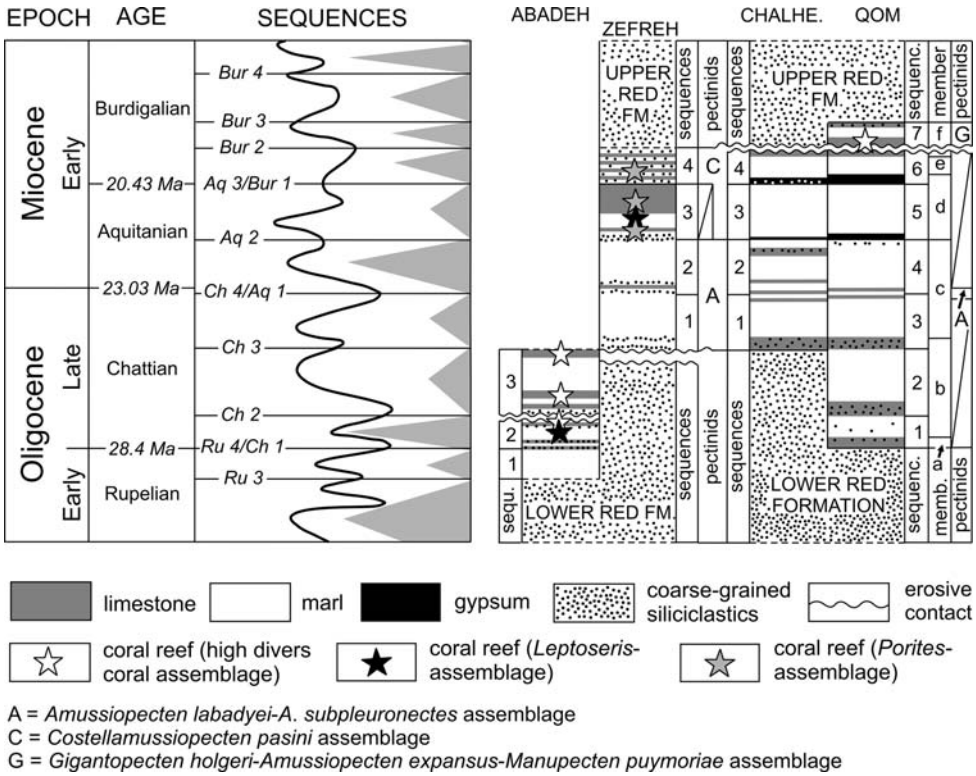

Fig. 11 Correlation chart of sedimentological events in the studied sections with the global sea-level curve of Hardenbol et al. (1998). Members refer to the lithostratigraphic scheme of Furrer and Soder (1955)

For sequence 4 an early Burdigalian age is indicated by the *Costellamussiopecten pasini* assemblage, as well as by the absence of the mid-Burdigalian *Gigantopecten holgeri–Amussiopecten expansus–Manupecten puymoriae* assemblage (Mandic and Steininnger 2003), which is, in turn, present in sequence 7 in the Qom section. Consequently, the four upper Rupelian to lower Burdigalian depositional sequences of Zefreh section correspond to the Ch 3 to Aq 3/Bur 1 sequences of Hardenbol et al. (1998).

Stratigraphic framework of the Qom back-arc basin

Two episodes of evaporation produced well traceable lithostratigraphic markers (gypsum beds) in the Qom and Chalheghareh areas that can be correlated with the d-Member of Furrer and Soder (1955). At both localities a unit of green marls follow above, which are covered by a unit of skeletal limestones that are equivalent with the e-Member (green marls) and the f-Member (skeletal limestones) of the lithostratigraphic scheme presented by Furrer and Soder (1955). This allows us to correlate the gypsum-bearing sequences 3 and 4 of the Chalheghareh section with sequences 5 and 6 of the Qom section, respectively (Fig. 11). Sequences 2 and 1 of section Chalheghareh are accordingly correlated with sequences 4 and 3 of section Qom, respectively.

This lithostratigraphic correlation is supported by biostratigraphy. The sections are pinpointed using microfossils at the Chattian/Aquitanian (sequences 3/4) and Aquitanian/Burdigalian (sequences 5/6) boundaries in the Qom section, as well as at the Chattian/Aquitanian boundary (sequences 1/2) in the Chalheghareh section. Age indications of a variety of faunal assemblages throughout the sections corroborate the correlation of the remaining sequences, which will be discussed in detail below.

In Qom section, the lower part of the b-Member (sequences 1–3) contains nannoplankton assemblages (beds 7 and 11) indicating a late Rupelian to Chattian age (NP24-NP25 of Martini 1971) due to the co-occurrence of *Reticulofenestra abisecta*, *R. bisecta*, and *Zygrhablithus bijugatus*. This age estimate is supported by a planktic foraminiferal fauna from bed 9, which includes *Globigerina angulioffícinalis*, *Gg. ciperoensis*, *Gg. labiacrassata*, *Gg. ouachitaensis*, and *Globigerinoides primordius*, also denoting a late Rupelian to early Chattian age. Lepidocyclinids from the middle subunit of the c-Member (lowstand of sequence 4) are represented by *Lepidocyclina* (*Nephrolepidina*) *morgani*-type and *L.* (*Eulepidina*) *dilatata* and point to a Chattian age. Therefore, the lower sequences 1–3 that span the Chattian are correlated with the Ru 4/Ch 1 (sequence 1), Ch 2 (sequence 2) and Ch 3 (sequence 3) cycles of Hardenbol et al. (1998).

The Oligo-/Miocene boundary is recognized between beds 29 and 30 in the lower part of sequence 4 [=Ch 4/Aq 1 cycle of Hardenbol et al. (1998)] because the succeeding marls contain the planktic foraminifers *Globigerina* cf. *ciperoensis*, *Globorotalia woodi*, *Globigerinoides primordius*, and *Gs. immaturus*, which characterize the Early Miocene.

The Aquitanian/Burdigalian boundary coincides with that of the d-/e-Member, as marls above the thick upper gypsum package (38) contain a diversified *Globigerinoides* assemblage [*Globigerinoides altiaperturus*, *Gs. immaturus*, *Gs. quadrilobatus*, *Gs. subquadratus*, *Gs. trilobus*, *Gs.* cf. *trilobus* ("*bisectus*" type), *Globoquadrina langhiana*, *Catapsydrax unicavus*, *Cassigerinella boudecensis*]. This assemblage is characteristic for the base of N5 according to Bolli and Saunders (1985), which is equivalent to the base of the *Globigerinoides altiaperturus–Catapsydrax dissimilis* Zone of Bizon and Bizon (1972) and Iaccarino (1985), and which defines the base of the Burdigalian in the Mediterranean. The Aquitanian/Burdigalian boundary corresponds with a sea-level lowstand (Aq 3/Bur 1) in the Hardenbol et al. (1998) sea-level curve (Fig. 11).

Nannoplankton assemblages from the lower (41) and upper part (52) of the e-Member (sequence 6) additionally indicate an Early Miocene age owing to the presence of *Sphenolithus* cf. *umbrellus*, *Helicosphaera* cf. *carteri*, and *Coccolithus* cf. *micropelagicus*, and the coeval absence of the typical Chattian forms *Reticulofenestra bisecta* and *Zygrhablithus bijugatus*.

For the f-Member in section Qom, a rich association of larger benthic foraminifers with *Borelis melo curdica*, *B. haueri*, *Peneroplis thomasi*, *P. armorica*, *Archaias* cf. *asmaricus*, *A. hensoni*, *A.* sp., and *Dendritina rangi* shows strong affinities to other Burdigalian faunas from the Middle East (Adams 1968; Ctyroky et al. 1975; Schuster and Wielandt 1999). Moreover, planktic assemblages from beds 102 to 108 (sequence 7) with *Globigerina dubia*, *Gg. lentiana*, *Gg. ottnangiensis*, *Gg. praebulloides*, *Cassigerinella boudecensis*, and *C. chipolensis* are similar to those of the mid-Burdigalian in the Mediterranean. The pectinid assemblage with *Gigantopecten holgeri*, *Amussiopecten expansus* and *Manupecten puymoriae*, which is characteristic for the upper part of the f-Member indicates a mid-Burdigalian age (Mandic and Steininger 2003). This assemblage neither occurs in the Zefreh sections nor in section Chalheghareh, which indicates a shorter stratigraphic range of these sections.

In section Chalheghareh, sequence 1 (beds 23–29) contains eu- and nephrolepidinids [*L.* (*E.*) *dilatata*, *L.* (*E.*) cf. *undulosa*, *L.* (*E.*) sp., *L.* (*Nephrolepidina*) spp.], which are regarded as Chattian in age. This assumption is supported by the associated planktic foraminifers (e.g.

Globigerina ouachitaensis, *Tenuitella munda*), indicating a mid- to Late Oligocene age (Schuster and Wielandt 1999). In addition, sequences 1 and 2 yield an *Amussiopecten subpleuronectes-A. labadyei* assemblage of late Chattian to early Aquitanian age.

Bed 56 (sequence 2) marks the base of the Aquitanian due to the first occurrence of *Miogypsinoides formosensis* and *M. bantamensis*. For the associated marls an Early Miocene age is indicated by planktic foraminiferal assemblages including *Globigerina praebulloides*, *Gg.* cf. *ottnangiensis*, *Globigerinoides primordius*, *Gs. immaturus*, *Gs. quadrilobatus*, and *Cassigerinella boudecensis*. While the Chattian/Aquitanian boundary is correlated with the lowstand of the Ch 4/Aq 1 cycle of Hardenbol et al. (1998), in section Chalheghareh the faunal assemblages at the boundary contradictorily indicate a relatively deep setting, which may suggest local tectonic movements of the nearby volcanic arc (Fig. 1b). Because sequence 2 is conformably overlying sequence 1, the former has to be equivalent with cycle Ch 3 of Hardenbol et al. (1998).

Finally, pectinid faunas in sequences 3 and 4 are characterized by *Costellamussiopecten pasini*, which suggests an Aquitanian to early Burdigalian age.

Integrating lithostratigraphic and biostratigraphic data, we correlate the bases of the upper gypsum deposits in the Qom and Chalheghareh sections (Fig. 8: bed 37 and Fig. 9: bed 95), with the Aquitanian/Burdigalian boundary. The Aq 3/Bur 1 cycle then corresponds to sequence 6 in Qom section and sequence 4 in Chalheghareh section, and the lower gypsum unit was formed at the beginning of the Aq 2 cycle (sequence 5 in Qom section, sequence 3 in Chalheghareh section).

Implications for the paleogeographic and paleobiogeographic evolution of the Tethyan Seaway

For the Esfahan-Sirjan and Qom basins, the gradual shifts from continental to offshore facies (and vice versa) indicate that sedimentation took place on extensive homoclinal ramps as already stated by Okhravi and Amini (1998) for the f-Member of the Qom Basin. The widespread occurrence of intertidal to shallow subtidal deposits and the absence of gravitative sediments (turbidites, slumps, etc.) indicate a gentle inclination of the ramps.

At first, the fore-arc basin was inundated by the marine transgression, of the Qom Sea during the late Early Oligocene (Ru 3 cycle), while in the back-arc basin marine environments were not established until the beginning of the Late Oligocene (Ru 4/Ch 1 cycle). Subsequently, normal marine conditions prevailed in both basins throughout the Oligocene (Fig. 12).

During the Early Miocene the situation changed because in the Qom back-arc basin the gates to the open ocean gradually became restricted due to the compressive tectonic regime, preventing water exchange between shallow landlocked areas and the open sea (Fig. 12). During the Aquitanian this process is displayed in the Qom Basin by the episodic precipitation of evaporites at sea-level lowstands at the beginning of the cycles Aq 2 and Aq 3/Bur 1. Uplift of the volcanic arc area caused by ongoing plate collision is shown by the emersion of the proximally positioned Chalheghareh and Zefreh sections already in the early Burdigalian (Bur 2). Final emersion of the Qom Basin is evidenced by deposition of the continental Upper Red Fm. during the mid-Burdigalian (Bur 3 cycle).

Shallow marine Oligo-/Miocene deposits also occur on the opposite side of the Tethyan Seaway along the African/Arabian coast. Sequences comparable to those of the Esfahan-Sirjan Basin are described from the Asmari Formation in the Iranian Zagros Basin (Seyrafian and Hamedani 1998; Vaziri-Moghaddam et al. 2006), which is part of the African/Arabian Plate. Sedimentation took place on a ramp-type carbonate platform (Vaziri-Moghaddam et al. 2006) and depositional environments include tidal flat, shelf lagoon, platform margin and open marine environments. Detailed descriptions and interpretations of the lithologies from the Asmari Fm. are given by Seyrafian and Hamedani (1998) and Vaziri-Moghaddam et al. (2006). For these Oligocene and Miocene sections the authors demonstrate that in most parts of the basin normal marine conditions prevailed and a restricted marine milieu was limited to marginal marine lagoons. However, in the NW Zagros Basin evaporitic deposits (Kalhur Member) locally interfinger with limestones of the middle Asmari Fm. (see Ala 1982), which has an Aquitanian age (Vaziri-Moghaddam et al. 2006) and may therefore be synchronous with evaporite formation in the Qom Basin. These evaporites precipitated in smaller, restricted areas of the Zagros Basin that formed due to the upthrust of the Zagros Mountains, which divided the Tethyan Seaway into several subbasins (Alsharhan and Nairn 1995) (Fig. 12).

For the uppermost Burdigalian part of the section in the north-central Zagros Basin, Seyrafian and Hamedani (1998) reconstructed increasingly restricted conditions. This development culminated in the deposition of the evaporitic Gachsaran Fm., which covers the Asmari Fm. basin-wide at the end of the Burdigalian (Ala 1982). At this time the continental milieu of the Upper Red Fm. was already installed in the Qom Basin and at least in marginal areas of the Esfahan-Sirjan Basin. The extensive distribution of terrestrial and hypersaline facies at the end of the Burdigalian in the area of the Tethyan Seaway points to separation of the Mediterranean and Indo-Pacific Tethys at this time.

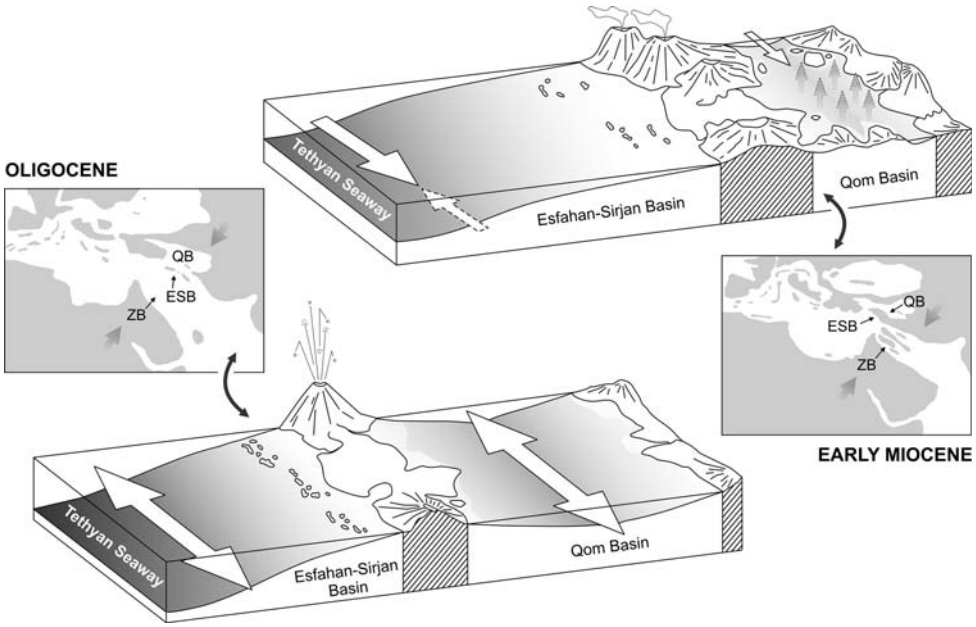

Fig. 12 Schematic block diagrams illustrating the development of the Esfahan-Sirjan Basin and Qom Basin from Late Oligocene to Early Miocene times (paleogeographic maps modified from Harzhauser and Piller 2007). The *black arrows* in paleogeographic maps tag the positions of the Zagros Basin (*ZB*), Qom Basin (*QB*) and Esfahan-Sirjan Basin (*ESB*); *white arrows* in block diagrams show the permeability of gateways. Oligocene: broad Tethyan Seaway and fully marine connections to the western Tethys via seaways to the north and south of Qom Basin. Early Miocene: restriction of the Tethyan Seaway, and closure of the gateways between Qom Basin and the Proto-Indopacific due to ongoing collission of Africa/Arabia with Eurasia, and upthrust of the Zagros mountain ranges. Transparent gray arrows indicate evaporation in the Qom Basin

However, in the Qom Basin a faunal turnover and change in faunistic relationships of pectinids already took place during the Bur 2 cycle (sequence 7 of Qom section) when the central seaway was still open. Whereas pectinid faunas from the a- to e-Members show a clear Indo-Pacific affinity until the early Burdigalian, f-Member pectinid faunas indicate a strong Mediterranean signal towards the mid-Burdigalian (Mandic 2000). The same development is shown by corals and gastropod faunas from the central Iranian Basins, in which Indo-Pacific elements diminish during the Early Miocene (Schuster and Wielandt 1999; Harzhauser et al. 2002; Harzhauser et al. 2007). This suggests that faunal exchange between the Qom Basin and the Indo-Pacific ceased, while at the same time the connectivity with the Mediterranean was enhanced. Even if Eurasia and Africa were not connected by a fully formed landbridge at this time, it is plausible that hypersaline waters in the shallow remaining Tethyan Seaway possibly formed a biogeographic barrier for Indo-Pacific marine biota shortly before the TTE.

Summary and conclusions

The Qom Formation was deposited on extended, mixed carbonate-siliciclastic, homoclinal ramps at the northeastern coast of the Tethyan Seaway in the Qom back-arc and Esfahan-Sirjan fore-arc basins (central Iran). It includes seven stratigraphic sequences that span the late Rupelian to mid-Burdigalian time interval and can be attributed to the Ru 3 to Bur 2 third order sea-level fluctuations of Hardenbol et al. (1998). The recognition and dating of these sequences in the Esfahan-Sirjan Basin and in the Qom Basin allows a basin-spanning stratigraphic correlation of the Qom Formation for the first time.

The elaborated stratigraphic scheme documents continuous restriction of the Tethyan Seaway with advanced collision of the African/Arabian and Eurasian/Iranian plates. For the Oligocene a normal marine milieu is displayed throughout the sedimentary successions of the fore- and back-arc basins. In the fore-arc basin these conditions endured during the Aquitanian and Early Burdigalian, while in the Qom Basin, as well as in other marginal basins on both coasts of the Tethyan Seaway, intermittent episodes with restricted marine conditions and emersions are documented. However, persisting gateways connecting the Qom Basin with the Mediterranean and Indo-Pacific sides of the Tethyan Seaway until the late Early Burdigalian is documented by Tethyan faunal elements from both sides of the Tethyan Seaway in the central Iranian basins. Yet after the Bur 2 lowstand emersion of the Qom Basin its recolonization occurred from the Mediterranean region only. Thus, the differentiation into an Atlantic-Mediterranean and an Indo-Pacific bioprovince took place before the final

paleogeographic disjunction of the Tethys (TTE), as shown by the comparison with the Zagros Basin, where marine sedimentation continued until the end of Burdigalian. It is therefore suggested that the continuous shallowing and restriction of the seaway generated an increasingly hostile hypersaline environment and a biogeographic barrier for marine biota.

Acknowledgments Our special thanks go to the other members of the research projects on Late Oligocene—Early Miocene circum-Mediterranean palaeobiogeographical relations, the project leaders F. F. Steininger (Eggenburg) and J. H. Nebelsick (Tübingen), as well as the researchers M.W. Rasser (Stuttgart), J. Reisinger (Korneuburg), F. Schuster (Freiburg), and J. Schlaf (Aberdeen). We also appreciate the comments from an anonymous reviewer. This work was supported by the Austrian FWF (P11886-GEO) and the Deutsche Forschungsgemeinschaft (STE 857/1-1; NE 537/1-1, -2).

References

Abaie IL, Ansari HJ, Badakhshan A, Jaafaki A (1963) History and development of the Alborz and Seraih fields, central Iran. In: Proc 6th world petrol conf, Frankfurt, pp 1–111

Adams CG (1968) A revision of the foraminiferal genus *Austrotrillina* Parr. Bull Brit Nat Hist Geol 16:73–97

Adams CG, Gentry AW, Whybrow PJ (1983) Dating the terminal Tethyan event. Utrecht Micropaleontol Bull 30:273–298

Ala MA (1982) Chronology of trap formation and migration of hydrocarbons in Zagros sector of southwest Iran. AAPG Bull 66:1536–1542

Alsharhan AS, Nairn AEM (1995) Tertiary of the Arabian Gulf: sedimentology and hydrocarbon potential. Palaeogeogr Palaeoclimatol Palaeoecol 114:369–384

Amidi SM (1983) Abadeh. Geological quadrangle map of Iran no. G9. Scale 1:250 000. Ministery of Mines and Metals and Geol Surv Iran

Amidi SM, Zahedi M (1991) Kashan. Geological quadrangle map of Iran no. F7. Scale 1:250 000. Ministery of Mines and Metals and Geol Surv Iran

Beavington-Penny SJ, Wright VP, Racey A (2006) The middle Eocene Seeb formation of Oman: an investigation of acyclicity, stratigraphic completeness, and accumulation rates in shallow marine carbonate settings. J Sed Res 76:1137–1161

Berggren WA, Kent DV, Aubry MP, Hardenbol J (1995) Geochronology, time scales and global stratigraphic correlation. SEPM Spec Publ 54:1–386

Bizon G, Bizon JJ (1972) Atlas des pincipaux foraminiféres planctoniques du basin méditerranéen. Oligocéne á quaternaire IX:1–316

Bolli HM, Saunders JB (1985) Oligocene to Holocene low latitude planktic foraminifera. In: Bolli HM, Saunders JB, Perch-Nielsen K (eds) Plankton stratigraphy. Cambridge University Press, London, pp 155–262

BouDhager-Fadel M, Banner FT (1999) Revision of the stratigraphic significance of the Oligo-Miocene "Letter-Stages". Rev Micropaleontol 42(2):93–97

Bozorgnia F (1966) Qum formation stratigraphy of the Central Basin of Iran and its intercontinental position. Bull Iran Petrol Inst 24:69–76

Cahuzac B, Poignant A (1997) Essai de biozonation de l'Oligo-Miocène dans les bassins europèens à l'aide des grands foraminifères nèritiques. Bull Soc Gèol Fr 168:155–169

Chahida MR, Papp A, Steininger F (1977) Fossilführung der Oligo/Miozänen Qum-formation in Profilen bei Abegarm-Zefreh bei Isfahan (Zentraliran). Beitr Paläont Österr 2:79–93

Coleman-Sadd SP (1982) Two stage continental collision and plate driving forces. Tectonophysics 90:263–282

Ctyroky P, Karim SA, van Vessem EJ (1975) *Miogypsina* and *Borelis* in the Euphrate limestone formation in the Western Desert of Iraq. N Jb Geol Paläont Abh 148:33–49

Emami MH (1991) Qom. Geological quadrangle map of Iran no. E6. scale 1:250 000. Ministery of Mines and Metals and Geol Surv Iran

Furrer MA, Soder PA (1955) The Oligo-Miocene formation in the Qum region (Iran). In: Proc IVth World Petroleum Congress, Roma, Italia

Hallock P (1985) Why are larger foraminifera large? Paleobiology 11:195–208

Hallock P, Glenn EC (1986) Larger foraminifera: a tool for paleoenvironmental analysis of Cenozoic carbonate depositional facies. Palaios 1:55–64

Hardenbol J, Thierry J, Farley MB, Jacquin T, De Gracianski PC, Vail PR (1998) Mesozoic and cenozoic sequence stratigraphic framework of European Basins. In: De Gracianski PC, Hardenbol J, Thierry J, Vail PR (eds) Mesozoic and cenozoic sequence stratigraphy of European basins. SEPM Spec Publ 60:3–14

Harzhauser M (2000) Paleobiogeography and Palecology of Oligocene and Lower Miocene Gastropods in the Eastern Mediterranean and the Western Indo-Pacific. PhD thesis, University of Vienna, p 259

Harzhauser M (2004) Oligocene gastropod faunas of the Eastern Mediterranean (Mesohellenic Trough/Greece and Esfahan-Sirjan Basin/Central Iran). Cour Forsch Inst Senckenberg 248:93–181

Harzhauser M, Piller WE (2007) Benchmark data of a changing sea—and events in the Central Paratethys during the Miocene. Palaeogeogr Palaeoclimatol Palaeoecol 253:8–31

Harzhauser M, Piller WE, Steininger FF (2002) Circum-mediterranean Oligo-/Miocene biogeographic evolution—the gastropods' point of view. Palaeogeogr Palaeoclimatol Palaeoecol 183:103–133

Harzhauser M, Kroh A, Mandic O, Piller WE, Göhlich U, Reuter M, Berning B (2007) Biogeographic responses to geodynamics: a key study all around the Oligo-Miocene Tethyan Seaway. Zool Anz 246:241–256

Iaccarino S (1985) Mediterranean Miocene and Pliocene planktic foraminifera. In: Bolli HM, Saunders JB, Perch-Nielsen K (eds) Plankton stratigraphy. Cambridge University Press, London, pp 283–314

Jones WR (1999) Marine invertebrate (chiefly foraminiferal) evidence for the paleogeography of the Oligocene-Miocene of Eurasia, and consequences for terrestrial vertebrate migration. In: Agusti J, Rook L, Andrews P (eds) Hominid evolution and environmental change in the Neogene of Europe. Cambridge University Press, London, pp 274–308

Kahng SE, Maragos JE (2006) The deepest, zooxanthellate scleractinian corals in the world? Coral Reefs 25:254

Mandic O (2000) Oligocene to early Miocene pectinid bivalves of Western Tethys (N-Greece, S-Turkey, Central Iran and NE-Egypt)—taxonomy and paleobiogeography. PhD thesis, University of Vienna, p 289

Mandic O, Steininger FF (2003) Computer-based mollusc stratigraphy—a case study from the Eggenburgian (Early Miocene) type region (NE Austria). Palaeogeogr Palaeoclimatol Palaeoecol 197:263–291

Martini E (1971) Standard tertiary and quaternary calcareous nannoplankton zonation, vol 2. In: Proc 2nd planktonic conf Roma, pp 739–785

Mostofi R, Gansser A (1957) The story behind the 5 Alborz. Oil Gas J 55:78–84

Nogole-Sadat MAA (1985) Les zones de decrochmentel Les virgations in Iran, consequences des resultats de LL de la region de Qom. Geol Surv Iran Rep 1–201

Okhravi R, Amini A (1998) An example of mixed carbonate-pyroclastic sedimentation (Miocene, Central Basin, Iran). Sediment Geol 118:37–54

Pedley M (1998) A review of sediment distributions and processes in Oligo-Miocene ramps of southern Italy and Malta (Mediterranean divide). In: Wright VP, Burchette TP (eds) Carbonate Ramps. Geol Soc Lond Spec Publs 149:163–179

Perrin C, Bosence D, Rosen B (1995) Quantitative approaches to paleozonation and paleobathymetry of corals and coralline algae in Cenozoic reefs. In: Bosence DWJ, Allison PA (eds) Marine palaeoenvironmental analysis from fossils. Geol Soc Lond Spec Publs 83:181–229

Rahaghi A (1973) Étude de quelque grands foraminiféres de la formation de Qum (Iran Central). Rev Micropal 16:23–38

Rahaghi A (1976) Contribution á l'étude de quelque grands foraminiféres de ÍIran. NIOC 6:1–79

Rahaghi A (1980) Tertiary faunal assemblage of Qum-Kashan, Sabzewar and Jahrum areas. NIOC 8:1–64

Robba E (1986) The final occlusion of Tethys: its bearing on Mediterranean benthic molluscs. Int Symp Shallow Tethys 2:405–426

Rögl F (1997) Paleogeographic considerations for Mediterranean and Paratethys Seaways (Oligocene to Miocene). Ann Naturhist Mus Wien 99A:279–310

Rögl F (1999) Mediterranean and Paratethys. Facts and hypotheses of an Oligocene to Miocene paleogeography (short overview). Geol Carpathica 50:339–349

Rögl F, Steininger FF (1983) Vom Zerfall der Tethys zu Mediterran und Paratethys. Ann Naturhist Mus Wien 85/A:135–163

Rögl F, Steininger FF (1984) Neogene Paratethys, Mediterranean and Indo-pacific seaways. In: Brenchley P (ed) Fossils and climate. Wiley, Chister, pp 171–200

Rosen BR, Aillud GS, Bosellini FR, Clack N, Insalaco E, Valldeperas FX, Wilson MEJ (2002) Platy coral assemblages: 200 million years of functional stability in response to the limiting effects of light and turbidity, vol 1. In: Proc 9th Int Coral Reefs Symp, Bali, pp 255–264

Rosenberg R (1975) Qum-1956: a misadventure in Iranian Oil. Bus Hist Rev 49:81–104

Schuster F, Wielandt U (1999) Oligocene and early Miocene coral faunas from Iran: paleoecology and paleobiogeography. Int J Earth Sci 88:571–581

Sen Gupta BK (1999) Foraminifera in marginal marine environments. In: Sen Gupta BK (ed) Modern foraminifera. Kluwer, Dordrecht, pp 141–159

Seyrafian A, Hamedani A (1998) Microfacies and depositional environment of the Upper Asmari formation (Burdigalian) North-Central Zagros Basin, Iran. N Jb Paläont Abh 210:129–141

Smith AM (1995) Palaeoenvironmental interpretation using bryozoans: a review. In: Bosence DWJ, Allison PA (eds) Marine palaeoenvironmental analysis from fossils. Geol Soc Lond Spec Publs 83:231–243

Stöcklin J, Setudehina A (1991) Stratigraphic lexicon of Iran. Geol Surv Iran Report 18, pp 1–376

Vaziri-Moghaddam H, Kimiagari M, Taheri A (2006) Depositional environment and sequence stratigraphy of the Oligo-Miocene Asmari formation in SW Iran. Facies 52:41–51

Wanless HR, Tedesco LP, Tyrell KM (1988) Production of subtidal tabular and surficial tempestites by Hurricane Kate, Caicos Platform, British West Indies. J Sediment Petrol 58:739–750

Wilson MEJ, Lokier SW (2002) Siliciclastic and volcaniclastic influences on equatorial carbonates: insights from the Neogene of Indonesia. Sedimentology 49:583–601

Whybrow PJ (1984) Geological and faunal evidence from Arabia for mammal migrations between Asia and Africa during the Miocene. Cour Forsch Inst Senckenberg 69:189–198

Woodroffe CD, Gagan MK (2000) Coral microatolls from the central Pacific record late Holocene El Niño. Geophys Res Lett 27:1511–1514

Zahedi M (1978) Esfahan. Geological quadrangle map of Iran no. J7. Scale 1:250 000. Ministery of Industry and Mines and Geol Surv Iran